On lepton flavour universality in semileptonic $B_c \to \eta_c, J/\psi$ decays

Domagoj Leljak,[a] **Blaženka Melić,**[a] **Monalisa Patra**[b]

[a]*Institut Rudjer Bošković, Division of Theoretical Physics, Bijenička 54, HR-10000, Croatia*
[b]*Jožef Stefan Institute, Jamova 39, P. O. Box 3000, 1001 Ljubljana, Slovenia*

ABSTRACT: We discuss $B_c \to \eta_c$ and $B_c \to J/\psi$ semileptonic decays within the Standard Model (SM) and beyond. The relevant transition form factors, being the main source of theoretical uncertainties, are calculated in the sum rule approach and are provided in a full q^2 range. We calculate the semileptonic branching fractions and find for the ratios, $R_{\eta_c}|_{\rm SM} = 0.32\pm0.02$, $R_{J/\psi}|_{\rm SM} = 0.23\pm0.01$. Both predictions are in agreement with other existing calculations and support the current tension in $R_{J/\psi}$ at 2σ level with the experiment. To extend the potential of testing the SM in the semileptonic B_c decays, we consider the forward-backward asymmetry and polarization observables. We also study the 4-fold differential distributions of $B_c \to J/\psi(J/\psi \to \tilde{\ell}^- \tilde{\ell}^+)\ell^- \bar{\nu}_\ell$, where $\tilde{\ell} = e, \mu$, in the presence of different new physics scenarios and find that the new physics effects can significantly modify the angular observables and can also produce effects which do not exist in the SM. Using the constraints on the new physics couplings from the recent combined analysis of BaBar, Belle and LHCb data on semileptonic $B \to D^{(*)}$ decays, where the effects of new physics could be visible, we find that these different new physics scenarios are not able to simultaneously explain the current experimental value of $R_{J/\psi}$.

Contents

1 Introduction

In September 2017 the LHCb collaboration announced the first measurement of testing the lepton flavor universality using charmed-beauty meson semileptonic decays to $J/\psi\tau^+\nu_\mu$ and $J/\psi\mu^+\nu_\mu$ [1]. The result for the measurement of the ratio of the branching fractions is

$$R_{J/\psi}|_{\exp} = \frac{BR(B_c^+ \to J/\psi\tau^+\nu_\tau)}{BR(B_c^+ \to J/\psi\mu^+\nu_\mu)} = 0.71 \pm 0.17 \pm 0.18, \tag{1.1}$$

and is more than 2σ away from the Standard model (SM) prediction. Currently there are many model dependent calculations of $R_{J/\psi}$ [2–14] within the SM and they give the results in the range (without including model uncertainties)

$$R_{J/\psi}|_{\rm SM} = 0.24 - 0.30, \tag{1.2}$$

However, the $R_{J/\psi}$ measurement is challenging. Due to the presence of invisible ν's, both decays are observed only through 3 muons, two of them coming from J/ψ decays and being perfectly identified. The third muon makes a difference and enables distinguishing the semileptonic B_c decays to τ and to μ from the background. Therefore it is still premature to speak about the new physics effects in these decays, although one can consider this probability having in mind that BABAR, Belle and LHCb have also found other intriguing anomalies in the semileptonic decays of B mesons, known as R_D and R_{D^*} [15–18]. These experimental collaborations have revealed a significant deviation of 2.3σ, and 3.5σ of the ratios R_D and R_{D^*} from the SM predictions. Also some deviations in $b \to s$ semileptonic decays are still present [19].

Moreover, calculations of these semileptonic heavy-meson decays involve theoretical uncertainties coming from imprecise determination of the hadronic transition form factors describing the hadronic effect in the transition from the initial to the final meson state.

The calculation of B_c form factors are difficult and leads to big uncertainties. If we summarize values of B_c into S-wave charmonia form factors at $q^2 = 0$ calculated in different models (perturbative QCD (pQCD) [2], three-point QCD sum rules (3ptQCDSR) [3, 4], light cone sum rules (LCSR) [5], relativistic quark model (RQM) [6–9], nonrelativistic quark models (NRQM) [10, 11], light-font quark model (LFQM) [12], constituent quark model (CQM)) [13], relativistic quark model (RCQM) [14]) in the literature we obtain:

$$f_+(0) = f_0(0) = 0.20 - 1.43, \tag{1.3}$$

for $B_c \to \eta_c$ form factors, and

$$\begin{aligned} V(0) &= 0.17 - 1.63, \\ A_1(0) &= 0.21 - 1.19, \\ A_2(0) &= 0.23 - 1.27, \\ A_0(0) &= 0.12 - 1.09, \end{aligned} \tag{1.4}$$

for $B_c \to J/\psi$ form factors. It is obvious that with such a large range of estimated form factors it is impossible to make any reliable prediction for R_{η_c} and $R_{J/\psi}$ ratios. Moreover, in many estimations of form factors, the theoretical errors were not given or they are not under control. Although some of the uncertainties cancel in the ratio, the model predictions of $R_{J/\psi}$ calculated in different approaches and taking the theoretical uncertainties into account vary in a huge range [20–25]

$$R_{J/\psi}|_{\mathrm{SM}} = 0.17 - 0.41. \tag{1.5}$$

The lattice QCD calculation for $B_c \to J/\psi$ form factors $V(q^2)$ and $A_1(q^2)$ are available now from the preliminary results of the HPQCD collaboration, at several points for $V(q^2)$ and $A_1(q^2)$ [26]. Earlier, the same collaboration has also produced results for $B_c \to \eta_c$ form factors, which were reported on in the same proceedings.

In this paper we will address the calculation of the form factors for $B_c \to S$-wave charmonia in the full q^2 range using the LCSR-inspired approach. The LCSR method was proven to be a reliable method for calculating transition form factors of many heavy-to light decays, such as $B_{(s)}, D_{(s)} \to \pi, \rho, K, K^*, \eta, \eta'$ [27–31] and even for $\Lambda_b \to \Lambda_c$ decays [32, 33]. We will compare our results with the existing QCD lattice points for $f_+(q^2)$ and $f_0(q^2)$ from $B_c \to \eta_c$ and $V(q^2)$ and $A_1(q^2)$ from $B_c \to J/\psi$ and will show the nice agreement, specially having in mind that the lattice results are still preliminary and do not include systematical errors. Following [22, 23] we have assigned 20% uncertainty to the lattice QCD results.

We also cite the results of our recent calculation derived by using the 3ptQCDSR method [4][1] and show that the form factors from two sum rule approaches, although calculated by using different quark-hadron duality assumptions, appear to be consistent and precise enough to enable precise determination of the ratios R_{η_c} and $R_{J/\psi}$ in the SM. Recently, there also appeared a model-independent estimation of the SM bounds on R_{η_c} and $R_{J/\psi}$ [22–24]. Such analysis rely on the data, available lattice results and the heavy-quark spin-symmetry (HQSS) relations for the form factors at the zero recoil and predict the R-ratios consistent with Eq.(1.2) and our calculation, clearly at 2σ discrepancy with the experiment. The HQSS and nonrelativistic QCD (NRQCD) relations used in these approaches will be carefully examined in Sec. 2.2.1.

The possible new physics (NP) effects in the semileptonic $B_c \to \eta_c(J/\psi)\ell\nu_\ell$ decays have been recently considered in the context of either specific models, such as the leptoquark models [34], left-right symmetric models, R-parity violating supersymmetric models, etc. [35–37] or in a model

---

[1]A very brief discussion on the 3ptQCDSR calculation is provided in Appendix A.

independent approach based on the most general effective Hamiltonian [20, 21, 25, 38–40]. To account for possible NP effects in $B_c \to \eta_c$ and $B_c \to J/\psi$ semileptonic decays we consider here the effective Hamiltonian approach consisting of all possible four-Fermi operators. The constraints on contributions of these NP operators and the corresponding Wilson coefficients are obtained from the experimental results of R_D, R_{D^*}, polarizations of τ and D^* in $B \to D^{(*)}l\nu$ decays, as well as on the B_c lifetime. There are various studies [41–46] performing a global fit on these NP operators considering the presence of only one or two NP operators simultaneously. We have taken the latest constraints on the Wilson coefficients from Ref. [43] and analysed the effects of these NP operators on various observables such as the ratio of the branching fractions, the forward-backward asymmetry, the convexity parameter and the longitudinal as well as the transverse polarization components of τ in the final state. We have also preformed the first study of the full 4-fold differential decay rate $B_c \to J/\psi \,(J/\psi \to \mu^+\mu^-, e^+e^-)l\nu_l$, where the leptons from the J/ψ decay are of opposite helicities. The 4-fold decay distribution in this case is proportional to three angles and the momentum transfer q^2. The three distinct angles gives the freedom to construct additional asymmetries which are sensitive to the real as well as the imaginary part of the new physics couplings.

The structure of the paper is as follows. We compute the form-factors in the context of our sum rule model in Sec. 2 and present the results in the whole q^2 range. We compare the results with those existing in the literature and with available preliminary lattice results. The discussion of the heavy-quark symmetry limit of form factors at the zero recoil is given in Sec. 2.2.1. The general effective Hamiltonian of the $b \to c\ell\nu_\ell$ transition is introduced in Sec. 3, and we obtain the semileptonic decay distributions for $B_c \to \eta_c, J/\psi$ in the presence of NP operators using the helicity technique. We compare predictions for different physical observables in the SM and in the presence of NP. A detailed comparison of predictions of $R_{\eta_c, J/\psi}$ in the SM, with the form factors calculated in our model, with the predictions from other approaches is also provided. In Sec. 4, we extend the calculation of $B_c \to J/\psi l\nu_l$ to the J/ψ decay into a pair of muons or electrons, and discuss the full 4-fold distribution. A set of new observables is considered and the results are compared for the SM case and beyond. Finally we conclude in the last section, Sec. 5.

2 Sum rule calculations for the form factors

We will perform the estimation of the $B_c \to \eta_c$ and $B_c \to J/\psi$ form factors using the LCSR-inspired method. We will follow the standard QCD sum rule method, by interpolating the B_c meson with an appropriate quark current and describing the S-wave charmonia by the distribution amplitudes (DAs) of an increasing twist.

The method of the LCSR is very well know and we will just briefly outline the procedure here in order to properly define all ingredients necessary for calculating the form factors. In the calculation we will use the following approximations: the twist-2 light-cone distribution amplitudes will be calculated in the NRQCD model [47], and the Gegenbauer polynomials expanded at the scale μ. The twist-3 and twist-4 DAs will be taken in their asymptotic form. Moreover, the Wandzura-Wilczek approximation will be applied, where the three-particle DA are neglected and therefore the twist-3 and twist-4 DAs are expressed in terms of the twist-2 distributions. The effects of the final state masses, m_{η_c} and $m_{J/\psi}$ are included [48].

The calculation of the form factors for $B_c \to \eta_c$ proceeds in a similar way as those for $B \to \pi, K$. [28, 30, 31, 49–52], while $B_c \to J/\psi$ form factor calculation closely follows the derivation of the form factors of $B \to K^*$ [29, 48, 51, 53, 54]. We have checked that with appropriate changes in the expressions, all our results agree with previous calculations.

2.1 Definitions

The form factors of the $B_c \to \eta_c$ decay are defined as

$$\langle \eta_c(p)|\bar{c}\gamma_\mu b|B_c(p_{B_c})\rangle = \left[(p+p_{B_c})_\mu - \frac{m_{B_c}^2 - m_{\eta_c}^2}{q^2}q_\mu\right]f_+(q^2) + \left[\frac{m_{B_c}^2 - m_{\eta_c}^2}{q^2}q_\mu\right]f_0(q^2),$$

$$\langle \eta_c(p)|\bar{c}\sigma_{\mu\nu}q^\nu b|B_c(p_{B_c})\rangle = \frac{i}{m_{B_c} + m_{\eta_c}}\left[q^2(p+p_{B_c})_\mu - (m_{B_c}^2 - m_{\eta_c}^2)q_\mu\right]f_T(q^2), \tag{2.1}$$

where $f_+(0) = f_0(0)$ and $0 \leq q^2 \leq (m_{B_c} - m_{\eta_c})^2$. The scalar form factor $f_0(q^2)$ follows also from the conservation of the vector current as

$$\langle 0|\bar{c}b|B_c(p_{B_c})\rangle = \frac{m_{B_c}^2 - m_{\eta_c}^2}{m_b(\mu) - m_c(\mu)}f_0(q^2). \tag{2.2}$$

The decay $B_c \to J/\psi \ell^+ \nu_l$ is described by the following form factors defined as [29]

$$\langle J/\psi(p,\epsilon)|\bar{c}\gamma_\mu(1-\gamma_5)b|B_c(p_{B_c})\rangle = -i\epsilon_\mu^*(m_{B_c} + m_{J/\psi})A_1(q^2) + i(p_{B_c}+p)_\mu(\epsilon^* \cdot q)\frac{A_2(q^2)}{m_{B_c}+m_{J/\psi}}$$

$$+ iq_\mu(\epsilon^* \cdot q)\frac{2m_{J/\psi}}{q^2}\left(A_3(q^2) - A_0(q^2)\right) + \varepsilon_{\mu\nu\rho\sigma}\epsilon^{*\nu}p_{B_c}^\rho p^\sigma \frac{2V(q^2)}{m_{B_c}+m_{J/\psi}} \tag{2.3}$$

where ϵ is the polarization vector of the J/ψ meson, $q = p_{B_c} - p$ is the momentum transfer varying in the range $0 \leq q^2 \leq (m_{B_c} - m_{J/\psi})^2$ and

$$A_3(q^2) = \frac{m_{B_c}+m_{J/\psi}}{2m_{J/\psi}}A_1(q^2) - \frac{m_{B_c}-m_{J/\psi}}{2m_{J/\psi}}A_2(q^2), \tag{2.4}$$

satisfying the relation

$$A_3(0) = A_0(0). \tag{2.5}$$

The form factor A_0 is the pseudoscalar form factor which can also be defined by applying the equation of motion to the derivative of the axial current:

$$\langle J/\psi|\bar{c}i\gamma_5 b|B_c\rangle = \frac{2m_{J/\psi}}{(m_b(\mu) + m_c(\mu))}(\epsilon^* \cdot q)A_0(q^2) \tag{2.6}$$

and, as it can be seen below, contributes to the $B_c \to J/\psi l\nu$ decay only if the lepton in the decay is considered to have a non-vanishing mass, which will be a case for the τ particle. The tensor form factors are usually defined as

$$\langle J/\psi(p,\epsilon)|\bar{c}\sigma_{\mu\nu}q^\nu(1+\gamma_5)b|B(p_{B_c})\rangle = 2i\varepsilon_{\mu\nu\rho\sigma}\epsilon^{*\nu}p_{B_c}^\rho p^\sigma T_1(q^2)$$

$$+ T_2(q^2)\left[\epsilon_\mu^*(m_{B_c}^2 - m_{J/\psi}^2) - (\epsilon^* \cdot q)(p_{B_c}+p)_\mu\right] + T_3(q^2)(\epsilon^* \cdot q)\left[q_\mu - \frac{q^2}{m_{B_c}^2 - m_{J/\psi}^2}(p_{B_c}+p)_\mu\right], \tag{2.7}$$

and

$$T_1(0) = T_2(0). \tag{2.8}$$

However, as discussed in [29, 48], in the standard QCD sum rule one has to consider the off-shell p_{B_c} momentum ($p_{B_c}^2 \neq m_{B_c}$) and in order to avoid any ambiguity in the interpretation of $p_{B_c}^2$

appearing at different steps of calculation it is more appropriate to use the following matrix element as a definition of the tensor form factors;

$$\langle J/\psi(p,\epsilon)|\bar{c}\sigma_{\mu\nu}\gamma_5 b|B(p_{B_c})\rangle = A(q^2)\left\{\epsilon^*_\mu(p_{B_c}+p)_\nu - (p_{B_c}+p)_\mu\epsilon^*_\nu\right\} - B(q^2)\left\{\epsilon^*_\mu q_\nu - q_\mu\epsilon^*_\nu\right\}$$
$$- 2C(q^2)\frac{\epsilon^*\cdot q}{m_{B_c}^2 - m_{J/\psi}^2}\left\{p_\mu q_\nu - q_\mu p_\nu\right\}. \tag{2.9}$$

where $A(q^2)$, $B(q^2)$ and $C(q^2)$ are related to $T_i(q^2)$ defined in Eq. (2.7) as

$$T_1(q^2) = A(q^2), \quad T_2(q^2) = A(q^2) - \frac{q^2}{m_{B_c}^2 - m_{J/\psi}^2}B(q^2), \quad T_3(q^2) = B(q^2) + C(q^2). \tag{2.10}$$

The form factors are extracted from the correlation function of the T-product of the weak current j_Γ, $\Gamma = V, A, S, P, T$ and an interpolating current of the B_c meson $j_{B_c} = m_b\bar{c}i\gamma_5 b$ among the vacuum and the external on-shell meson M ($M = J/\psi, \eta_c$),

$$\Pi(q^2, p_{B_c}^2) = i\int d^4x e^{iqx}\left\langle M(p)\left|T\left\{j_\Gamma(x)j_{B_c}^\dagger(0)\right\}\right|0\right\rangle. \tag{2.11}$$

Both $B_c \to M$ decays proceed through b-quark decays and we assume that in the region of the large $m_b^2 - q^2 \leq \mathcal{O}(m_b\Lambda_{QCD})$ and $m_b^2 - p_{B_c}^2 \leq \mathcal{O}(m_b\Lambda_{QCD})$ virtualities, the correlation function Eq. (2.11) are dominated by the light-like distances and the description in terms of the products of perturbatively calculable hard-scattering kernels with non-perturbative and universal light-cone distribution amplitude (LCDA), ordered by increasing twist, is appropriate.

By inserting the sum over states with B_c quantum numbers and by using

$$\langle 0|j_{B_c}|B_c(p_B)\rangle = \frac{f_{B_c}m_{B_c}^2}{m_b(\mu) + m_c(\mu)} \tag{2.12}$$

for the ground state, with the use of hadronic dispersion relation in the virtuality $p_{B_c}^2$ of the B_c channel, we can relate the correlation function Eq. (2.11) to the $B_c \to M$ matrix elements and the form factors defined above. As usual, the quark-hadron duality is used to approximate heavier state contribution by introducing the effective threshold parameter $s_0^{B_c}$ and the ground state contribution of the B_c meson is enhanced by the Borel transformation in the variable $p_{B_c}^2 \to \sigma^2$.

The strategy which we use to fix the sum rule parameters, in particular the continuum threshold parameter $s_0^{B_c}$, is to use the lattice results for the decay constant of B_c, Eq. (2.18) and fix the continuum threshold parameters by calculating the constant with the 2-point functions calculated in the LCSR. This is done by using the NLO expression and the pole m_b, m_c masses. The $\overline{MS}$ masses used in the paper are taken as $m_b(\overline{m_b}) = 4.18$ GeV and $m_c(\overline{m_c}) = 1.27$ GeV. We have achieved the stability of the sum rules, i.e. that continuum and higher-order corrections are suppressed and that also the mass of B_c is correctly reproduced for $\mu = 3.9 \pm 0.3$ GeV. With the calculated $s_0^{B_c} = 46.8 \pm 0.8$ GeV^2 we have also checked the stability of the sum rules for $B_c \to M$ transitions. In both cases, the results are very stable on the variation of the Borel parameter, allowing σ^2 to vary between $70 - 90\,\text{GeV}^2$ with almost no change. Other parameters used in the paper are taken from the lattice results or from the NRQCD models described afterwards.

The method of the LCSR was extensively used for calculating the heavy-to-light transition form factors. Here the situation is far more complicated since the final meson is a quarkonium state η_c or J/ψ. Therefore, to properly account for the non-negligible large mass corrections $\mathcal{O}(2m_c)$ in the correlator, one would have to do a systematic expansion of the correlator near the light cone including those corrections. This is a highly nontrivial task and according to our knowledge has not been done yet. In the future, to improve the whole picture, one has to do a revised consideration of the LCDA for charmonia, similar to what was done for heavy hadrons (B-mesons and Λ_b), by

proving the factorization theorems and deriving the RG evolution kernels of LCDA by considering full mass corrections. But, such a calculation for charmonia is far more complicated since there is no help from HQET and heavy-quark symmetries, neither can one achieve fast convergence in the heavy-mass expansion. Such a calculation, if consistently doable for charmonia, is far beyond the scope of our paper. Here we assume that these potentially large intrinsic mass effects can be effectively described using proper phenomenological model of DAs. So, we will follow a simplified sum rule model where we treat charmonia of B_c-decays as light particles in the correlator (2.11) expansion near the light-cone and will closely follow the approach of the standard LCSR in what follows. On the other hand, to describe nonperturbative properties of charmonia we will use the NRQCD-inspired DAs which exactly reproduce leading NR moments of charmonia at ~ 1 GeV energies. To resolve the right DA structure at the $\sim m_b$ energies of the decay, we calculate the Gegenbauer expansion and evolution of DAs. The corrections to the leading approximation will be done by making the twist-expansion and by taking the large m_c mass correction in twist-3 and twist-4 DAs into account. The genuine $\mathcal{O}(4m_c^2/m_b\Lambda_{QCD})$ corrections are not included as we assume the collinearity of the wave functions. Moreover, since we are aware of our model constraints in describing charmonia particles, we will show the stability of the model on the variation of parameters of the model, the consistency of our results with the 3ptSR calculation of the same form factors done with the same parameters used here and will also show consistency of the calculated form factors with the HQSS/NRQCD symmetry relations among form factors.

The leading twist-2 DA of a η_c meson is defined as follows [55]

$$\langle 0|\bar{c}(z)\gamma_\mu\gamma_5[z,-z]c(-z)|\eta_c(p)\rangle = -if_{\eta_c}p_\mu\int_{-1}^{1}d\xi e^{i\xi pz}\phi(\xi,\mu), \tag{2.13}$$

while for the J/ψ we have

$$\langle 0|\bar{c}(z)\gamma_\mu[z,-z]c(-z)|J/\psi(p,\epsilon^{(\lambda=0)})\rangle = f_{J/\psi}m_{J/\psi}p_\mu\int_{-1}^{1}d\xi e^{i\xi px}\phi_{||}(\xi,\mu),$$

$$\langle 0|\bar{c}(z)\sigma_{\mu\nu}[z,-z]c(-z)|J/\psi(p,\epsilon^{(\lambda=\pm1)})\rangle = if_{J/\psi}^\perp(\epsilon_\mu p_\nu - \epsilon_\nu p_\mu)\int_{-1}^{1}du e^{i\xi px}\phi_\perp(\xi,\mu), \tag{2.14}$$

where $[z,-z] = P\exp\left\{ig\int_{-z}^{z}dx^\mu A_\mu(x)\right\}$ is a gauge integral. In above $\xi = u - (1-u)$, u is a fraction of a longitudinal momentum of a meson M carried by a c-quark and $(1-u)$ is a fraction of momentum carried by the c-antiquark. The DAs is defined at a scale μ at which the transverse momenta are integrated up to and all momenta below are included in the nonperturbative DAs ϕ. Other higher-twist amplitudes and higher-order corrections are defined similarly. For all details see, for example [48]. The vector and tensor decay constants $f_{J/\psi}$ and $f_{J/\psi}^T$ are defined as

$$\langle 0|\bar{c}(0)\gamma_\mu c(0)|J/\psi(p,e^{(\lambda)})\rangle = f_{J/\psi}m_{J/\psi}e_\mu^{(\lambda)},$$
$$\langle 0|\bar{c}(0)\sigma_{\mu\nu}c(0)|J/\psi(p,e^{(\lambda)})\rangle = if_{J/\psi}^T(\mu)(e_\mu^{(\lambda)}p_\nu - e_\nu^{(\lambda)}p_\mu), \tag{2.15}$$

where $f_{J/\psi}^T$ is renormalization scale dependent:

$$f_{J/\psi}^T(\mu'^2) = \left(\alpha_s(\mu'^2)/\alpha_s(\mu^2)\right)^{C_f/\beta_0}f_{J/\psi}^T(\mu) \tag{2.16}$$

and $\beta_0 = 11 - 2/3n_f$, n_f being the number of flavors involved. The decay constant for η_c is defined correspondingly as

$$\langle 0|\bar{c}\gamma_\mu\gamma_5 c|\eta_c(p)\rangle = -if_{\eta_c}p_\mu. \tag{2.17}$$

For the decay constants we will use the lattice results

$$f_{B_c} = 0.427(6)(2)\,\text{GeV}\ [56,\,57],$$
$$f_{J/\psi} = 0.405(6)(2)\,\text{GeV}\ [58],$$
$$f_{\eta_c} = 0.3947(24)\,\text{GeV}\ [59], \tag{2.18}$$

while for $f_{J/\psi}^T$ we will use the value extracted from the ratio

$$R_{J/\psi}^T = \frac{f_{J/\psi}^T(\mu = 2\ \text{GeV})}{f_{J/\psi}} = 0.975 \pm 0.010, \tag{2.19}$$

derived by considering combined QCDSR and lattice results [60]. The predictions for charmonia decay constants in [60] also nicely agree with the lattice results above.

2.1.1 Distribution amplitudes for charmonia

The leading twist-2 DAs are expanded in terms of Gegenbauer polynomials as:

$$\phi_P(u,\mu^2) = 6u(1-u)\left(1 + \sum_{n=1}^{\infty} a_n^P(\mu^2) C_n^{3/2}(2u-1)\right). \tag{2.20}$$

The leading term is the asymptotic form $\phi(u,\mu^2 \to \infty) = 6u(1-u)$. The Gegenbauer coefficients a_n are renormalized multiplicatively

$$a_n^P(Q^2) = \left(\alpha_s(Q^2)/\alpha_s(\mu^2)\right)^{\gamma_n^P/(2\beta_0)} a_n^P(\mu^2), \tag{2.21}$$

where the anomalous dimensions $\gamma_n^{\|,\perp}$ are given by

$$\gamma_n^{\|} = 8C_F\left(\sum_{k=1}^{n+1} 1/k - \frac{3}{4} - \frac{2}{(n+1)(n+2)}\right), \tag{2.22}$$

$$\gamma_n^{\perp} = 8C_F\left(\sum_{k=1}^{n+1} 1/k - 1\right). \tag{2.23}$$

Here $C_F = (N_c^2 - 1)/(2N_c)$ and $\beta_0 = 11/3N_c - 2/3N_f$, in which N_c is the number of colors and N_f the number of flavors. The coefficients $a_n^{\|}$ appear in $\phi(\xi,\mu)$ and $\phi_{\|}(\xi,\mu)$, while $a_n^{\perp}$ are coefficients in the expansion of the transversal twist-2 DA $\phi_{\perp}(\xi,\mu)$ of a J/ψ meson.

The Eq. (2.20) can be inverted to give the coefficients of the conformal expansion

$$a_n^P(\mu) = \frac{2(2n+3)}{3(n+1)(n+2)} \int_0^1 du\, C_n^{(3/2)}(2u-1)\, \phi_P(u,\mu), \tag{2.24}$$

and with the help of these coefficients at some low-energy scale μ_0, the DA $\phi_P(\xi,\mu)$ can be reconstructed at any scale μ.

The distribution amplitudes can also be defined with the help of calculated moments of DAs at some scale μ as

$$\langle \xi^n \rangle_\mu = \int_{-1}^{1} d\xi\, \xi^n \phi(\xi,\mu). \tag{2.25}$$

Charmonia particles are flavor-symmetric and therefore their DAs are symmetric around $u = 1/2$. The second moment is calculated in NRQCD [61, 62]

$$\langle \xi^2 \rangle_{\mu_0} = \frac{\langle v^2 \rangle_M}{3} + \mathcal{O}(v^4), \tag{2.26}$$

where $\mu_0 \sim 1\text{GeV}$.

The values of the nonrelativistic speeds v^2 of quarks in η_c and J/ψ mesons are obtained in NRQCD by including the first-order α_s corrections and non-perturbative contributions proportional to v^2 in the analysis of $\Gamma(\eta_c \to \gamma\gamma)$ and $\Gamma(J/\psi \to e^+e^-)$ rates, respectively, and $\langle v^2 \rangle_{J/\psi} = 0.225\,^{+0.106}_{-0.088}$ [47], $\langle v^2 \rangle_{\eta_c} = 0.226\,^{+0.123}_{-0.098}$ [47], $\langle v^2 \rangle_{J/\psi} = \langle v^2 \rangle_{\eta_c} = 0.21 \pm 0.02$ [62, 63] have been extracted. As stated in [64], the two-loop [65, 66] and three-loop [67] perturbative corrections to the NRQCD predictions for the $\Gamma(J/\psi \to e^+e^-)$ decay rate is known to be large. In [68] and [69] the $\mathcal{O}(v^2)$ and $\mathcal{O}(\alpha_s)$ corrections to twist-2 DAs of η_c and J/ψ have been calculated. At leading order approximation in relative velocity v there is no difference between η_c and J/ψ mesons and the results for the moments obtained are valid for both charmonia DAs. Based on the power-counting rules of NRQCD one would naively expect that $\langle v^2 \rangle \sim 0.3$. Taking all above into account, we will use the latest improved value [47, 70, 71] for both charmonia:

$$\langle v^2 \rangle = 0.201 \pm 0.064. \tag{2.27}$$

For the model of twist-2 DA at $\mu_0 = 1$ GeV we adopt the Gaussian model [64]:

$$\phi(u, \mu_0) = N_\sigma \frac{4u(1-u)}{\sqrt{2\pi}\sigma} \exp\left[-\frac{(u-\frac{1}{2})^2}{2\sigma^2}\right]; \qquad \sigma^2 = \frac{\langle v^2 \rangle_M}{12}, \tag{2.28}$$

where $N_\sigma \approx 1$ is the normalization constant defined from

$$\int_{-1}^{1} d\xi \, \phi(\xi, \mu) = 1. \tag{2.29}$$

We also use the Wandzura-Wilczek approximation where three-particle twist-3 DAs containing quarks and a gluon are neglected. In that case the twist-3 DAs of η_c are fixed to their asymptotic forms including mass corrections [72]:

$$\begin{aligned}
\phi_p(u, \mu)\big|_{\text{WWA}} &= 1 + \rho_+(\mu)\phi_{p,+}(u, \mu), \\
\phi_\sigma(u, \mu)\big|_{\text{WWA}} &= 6u(1-u) + \rho_+(\mu)\phi_{\sigma,+}(u, \mu),
\end{aligned} \tag{2.30}$$

where $\rho_+(\mu) = 4m_c^2(\mu)/m_{\eta_c}^2$ and

$$\begin{aligned}
\phi_{p,+}(u, \mu) &= \frac{1}{4}\left[\int_0^u dv \frac{\phi'(v, \mu)}{1-v} - \int_u^1 dv \frac{\phi'(v, \mu)}{v}\right], \\
\phi_{\sigma,+}(u, \mu) &= -\frac{3}{2}u(1-u)\left[\int_0^u dv \frac{\phi(v, \mu)}{(1-v)^2} + \int_u^1 dv \frac{\phi(v, \mu)}{v^2}\right].
\end{aligned} \tag{2.31}$$

For the J/ψ meson the situation is somewhat more complicated. In the Wandzura-Wilczek approximation where three-particle DAs are neglected, by using equations of motion the twist-3 DAs can be expressed in terms of the leading twist-2 DAs $\phi_{\parallel,\perp}$ with the valence quark mass corrections

$$\delta_+(\mu) = \frac{2m_c(\mu)}{m_{J/\psi}}\frac{1}{R_{J\psi}^T}, \quad \tilde{\delta}_+(\mu) = \frac{2m_c(\mu)}{m_{J/\psi}}R_{J\psi}^T, \tag{2.32}$$

as [27, 73–76]:

$$\tilde{h}_{\parallel}^{(s)} = (1 - \delta_+(\mu))h_{\parallel}^{(s)}, \qquad \tilde{g}_{\perp}^{(a)} = (1 - \tilde{\delta}_+(\mu))g_{\perp}^{(a)},$$

and

$$g_\perp^{(v)}(x,\mu)\big|_{\text{WWA}} = \frac{1}{4}\left[\int_0^u dv\,\frac{\Phi_{||}(y,\mu)}{1-v} + \int_u^1 dv\,\frac{\Phi_{||}(v,\mu)}{v}\right] + \tilde{\delta}_+(\mu)\phi_\perp(u,\mu), \tag{2.33}$$

$$\tilde{g}_\perp^{(a)}(x,\mu)\big|_{\text{WWA}} = (1-u)\int_0^u dv\,\frac{\Phi_{||}(v,\mu)}{1-v} + u\int_u^1 dv\,\frac{\Phi_{||}(v,\mu)}{v}, \tag{2.34}$$

$$h_{||}^{(t)}(u,\mu)\big|_{\text{WWA}} = \frac{1}{2}\xi\left[\int_0^u dv\,\frac{\Phi_\perp(y,\mu)}{1-v} - \int_u^1 dv\,\frac{\Phi_\perp(v,\mu)}{v}\right] + \delta_+(\mu)\phi_{||}(u,\mu), \tag{2.35}$$

$$\tilde{h}_{||}^{(s)}(u,\mu)\big|_{\text{WWA}} = (1-u)\int_0^u dv\,\frac{\Phi_\perp(v,\mu)}{1-v} + u\int_u^1 dv\,\frac{\Phi_\perp(v,\mu)}{v}, \tag{2.36}$$

with

$$\Phi_{||}(u) = 2\phi_{||}(u) + \tilde{\delta}_+\xi\phi_\perp'(u),$$
$$\Phi_\perp(u) = 2\phi_\perp(u) - \delta_+\left(\phi_{||}(u) - \frac{\xi}{2}\phi_{||}'(u)\right). \tag{2.37}$$

The J/ψ twist-4 DAs will be taken in their asymptotic form:

$$h_{\perp,3} = 6u(1-u),\quad g_{||,3} = 6u(1-u),$$
$$A_{||} = 24u^2(1-u)^2,\quad A_\perp = 12u^2(1-u)^2. \tag{2.38}$$

Some comments are in order. In the $B_c \to \eta_c$ decay we will retain only contributions up to twist-3 terms. It is well known that the standard twist expansion works very well for $B \to$ pseudoscalar form factors. It could be that in our case, for $B_c \to \eta_c$, twist-4 corrections are somewhat larger, due to the large and non-negligible m_c mass, but since hadronic parameters for the twist-4 contribution for η_c are not known we will not include them. In the decay $B_c \to J/\psi$ we keep all contributions up to twist-4, since their asymptotic form does not depend on the hadronic parameters. The J/ψ DAs defined above do not correspond to matrix elements of operators with definite twist [29]: $\phi_{\perp,||}$ are of twist-2, $h_{||}^{(s,t)}$ and $g_\perp^{(v,a)}$ contain a mixture of twist-2 and 3 contributions and $A_{\perp,||}$, h_3, g_3 are a mixture of twist-2, 3 and 4 contributions. Therefore it is usual to refer to $g_\perp^{(v,a)}$, $h_{||}^{(s,t)}$ as twist-3 LCDAs and to h_3, g_3, $A_{\perp,||}$ as twist-4 LCDAs. Also, as the mass of the vector particle in $B \to$ vector decays plays a significant role, in [29] it was proposed the following classification of relevance in the two-particle LCDA: $O(\delta^0): \phi_\perp; O(\delta^1): \phi_{||}, g_\perp^{(v,a)}; O(\delta^2): h_{||}^{(s,t)}, h_3, A_\perp; O(\delta^3): g_3, A_{||}$, where now $\delta \sim m_{J/\psi}$ is treated as an expansion parameter. For more detailed discussion see [48, 51, 53].

2.2 Parametrization of the form factors and the results

The derivation of the sum rule expressions for the form factors proceeds in a standard way [48, 51, 53, 54].

The general expression for the calculation of the form factors is given by

$$F_{B_c\to M}(q^2) = \frac{m_b + m_c}{m_{B_c}^2 f_{B_c}} e^{m_b^2/\sigma^2} \int_{u_0^{B_c}}^1 \frac{du}{u} \exp\left[-\frac{m_b^2 - \bar{u}q^2 - u\bar{u}m_M^2}{u\sigma^2}\right] F(u,\mu,q^2), \tag{2.39}$$

where

$$u_0^{B_c} = \frac{1}{2m_M^2}\sqrt{(s_0^{B_c} - q^2 - m_M^2)^2 + 4m_M^2(m_b^2 - q^2)} - (s_0^{B_c} - q^2 - m_M^2), \tag{2.40}$$

σ is a Borel parameter and $\bar{u} = 1 - u$. The functions $F(u,\mu,q^2)$ contain all twist contributions in terms of the various twist DAs, and the higher-twist contributions are suppressed by the Borel parameter.

The derived results at $q^2 = 0$ are listed in Table 1, together with the recent QCDSR result [4] briefly discussed in Appendix A and earlier results found in the literature on the same form factors. The errors are obtained by varying all parameters in a given range and adding them in quadratures.

Form Factor	this work [2]	QCDSR [4]	QCDSR [3]	SR [5]	pQCD [2]	CCQM [25, 77]	RQM [9]	RQM [8]	LFQM [12]	latt. [26]
$f_{+,0}^{\eta_c}(0)$	0.62 ± 0.05	0.41 ± 0.04	0.66	0.87	0.48(7)	0.75	0.47	0.54	0.61(5)	0.59
$V^{J/\psi}(0)$	0.73 ± 0.06	0.70 ± 0.06	1.03	1.69	0.42(2)	0.78	0.49	0.73	0.74(4)	0.70
$A_1^{J/\psi}(0)$	0.55 ± 0.04	0.50 ± 0.05	0.63	0.75	0.46(3)	0.56	0.50	0.52	0.50(3)	0.48
$A_2^{J/\psi}(0)$	0.35 ± 0.03	0.43 ± 0.05	0.69	1.69	0.64(3)	0.55	0.73	0.51	0.44(5)	-
$A_0^{J/\psi}(0)$	0.54 ± 0.04	0.53 ± 0.04	0.60	0.27	0.59(3)	0.56	0.40	0.53	0.53(3)	-
$f_T^{\eta_c}(0)$	0.93 ± 0.07	-	-	-	-	0.93	-	-	-	-
$T_{1,2}^{J/\psi}(0)$	0.47 ± 0.04	0.48 ± 0.03	-	-	-	0.56	-	-	-	-
$T_3^{J/\psi}(0)$	0.19 ± 0.01	0.27 ± 0.03	-	-	-	0.20	-	-	-	-

Table 1: Form factor predictions at $q^2 = 0$. Recent relevant lattice results are given by the HPQCD collaboration [26], reported here in orange, without the systematical error.

It is well know that the form factors extracted from the sum rules are valid in the low q^2 region. We use our results for the form factors and calculate them in the range $q^2 = \{-5, 5\}$ GeV. Then we extrapolate them from the low q^2 region to the q^2_{max} by using Bourrely-Caprini-Lellouch (BCL) parametrization [78] of the form factor series expansion in powers of a conformal mapping variable, which satisfies unitarity, analyticity and perturbative QCD scaling. The BCL parametrization is based on a rapidly converging series in the parameter z as

$$f(t) = \frac{1}{P(t)} \sum_{k=0} \alpha_k z^k(t, t_0),$$
$$z(t, t_0) = \frac{\sqrt{t_+ - t} - \sqrt{t_+ - t_0}}{\sqrt{t_+ - t} + \sqrt{t_+ - t_0}}, \tag{2.41}$$

weighted by a simple pole function $P(q^2) = 1 - t/m_R^2$ which accounts for low-laying resonances present below the threshold production of real $B_c - M$ pairs at $t_+ = (m_{B_c} + m_M)^2$. The parameter t_0, $0 \le t_0 \le t_- = (m_{B_c} - m_M)^2$ is a free parameter that can be used to optimize the convergence of the series expansion. For the truncation to only two terms in expansion Eq. (2.41), it was shown that the optimized value of t_0 has the form [79]:

$$t_{0|opt} = t_+ \left(1 - \sqrt{1 - \frac{t_-}{t_+}}\right). \tag{2.42}$$

and that the other choices of t_0 do not make a visible change in the form factors parametrization.

Masses of resonances appearing in the fits are determined by the properties of the form factors. The form factors V and T_1 correspond to the vector components of the currents, and, as the B_c meson is a pseudoscalar, they correspond to the axial vector components of the matrix elements. $A_{1,2}$, as well as $T_{2,3}$, correspond to the axial vector component of the $V - A$, while the form factor A_0

---

[2] The cited errors are obtained just by varying all parameters of the model and their smallness shows the stability of the sum rules used to obtain the predictions for the form factors. The errors do not include intrinsic uncertainties of the model itself which are hard to predict and could potentially increase the errors and lower the accuracy of the predictions.

correspond to the pseudoscalar current and only contributes in the decays with the non-vanishing lepton masses (in the semileptonic B_c decays with the τ lepton in our case). All relevant resonance masses are given in Table 2, together with the fitted parameters α_0, α_1 from Eq. (2.41).

The predicted form factors in a full q^2 range are shown in Figs. 1, 2, 3.

Form factor	J^P	m_R (GeV)	α_0	α_1
f_+	1^-	6.34	0.62	-6.13
f_0	0^+	6.71	0.63	-4.86
f_T	1^-	6.34	0.93	-9.36
V	1^-	6.34	0.74	-8.66
A_1	1^+	6.75	0.55	-4.67
A_2	1^+	6.75	0.35	-1.78
A_0	0^-	6.28	0.54	-6.80
T_1	1^-	6.34	0.48	-4.88
T_2	1^+	6.75	0.48	-2.93
T_3	1^+	6.75	0.19	-1.69

Table 2: Summary of the BCL fit for $B_c \to \eta_c$ and $B_c \to J/\psi$ form factors. The masses of the low-laying B_c resonances are taken from [80–83]
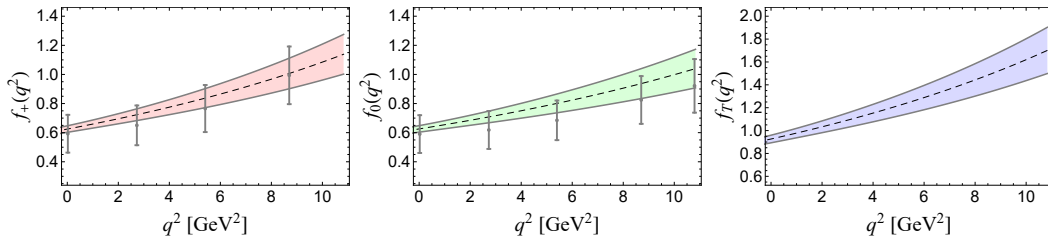

Figure 1: Pseudoscalar form factors for $B_c \to \eta_c$ calculated in this paper, including the lattice points from [26] with added 20% systematical error.

2.2.1 HQSS/NRQCD symmetry relations among from factors at the zero recoil

It is interesting to check the HQSS and NRQCD limits of the form factors for $B_c \to \eta_c$ and $B_c \to J/\psi$ decays. These decays are specific since the decay proceeds through $b \to c$ quark decay and the produced final state is a particle formed by two c quarks. And although they look like as a heavy-to-heavy transitions and produce interesting symmetries in a heavy-quark limit [84], the c-quark is significantly lighter than b and the produced c-quark is quite energetic, which spoils exact heavy-flavor symmetries. On the other hand c-quark is heavy enough that such decays can be considered as nonrelativistic so that the approximation of the zero-recoil point, i.e. the symmetry relations for a maximum momentum transfer $q^2_{\max} = (m_{B_c} - m_{J/\psi, \eta_c})^2$ still hold and the form factors can be related to a single function Δ [84–86], with an unknown normalization. Following [84] we write for the form factors near zero recoil ($q' \ll m_c$):

$$\langle \eta_c(v, q')| V_\mu(q^2) |B_c(v)\rangle = 2\sqrt{m_{B_c} m_{\eta_c}}\, \Delta(a_0 q')\, v_\mu, \qquad (2.43)$$

$$\langle J/\psi(v, q')| A_\mu(q^2) |B_c(v)\rangle = 2\sqrt{m_{B_c} m_{J/\psi}}\, \Delta(a_0 q')\, \epsilon^*_\mu, \qquad (2.44)$$

where $V_\mu = \bar{b}\gamma_\mu c$ and $A_\mu = \bar{b}\gamma_\mu\gamma_5 c$ and ϵ_μ is a polarization vector of J/ψ. Here v is the velocity of the B_c meson, and q' is a small residual velocity carried by the final state meson (not to be confused
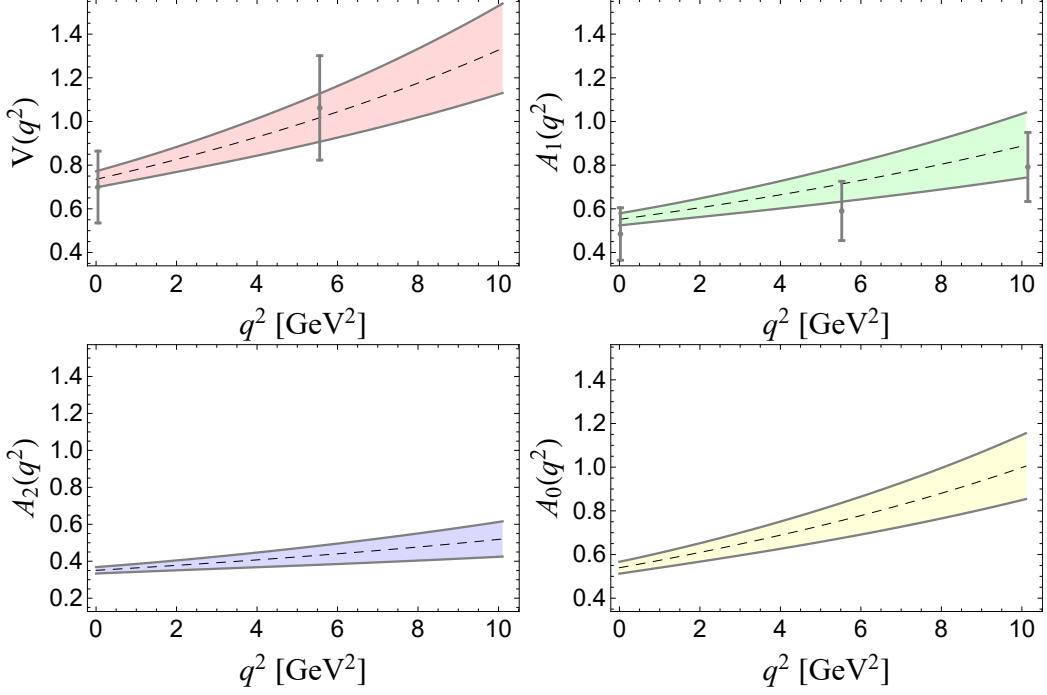
Figure 2: SM form factors for $B_c \to J/\psi$ calculated in this paper, including the lattice points from [26] with added 20% systematical error.
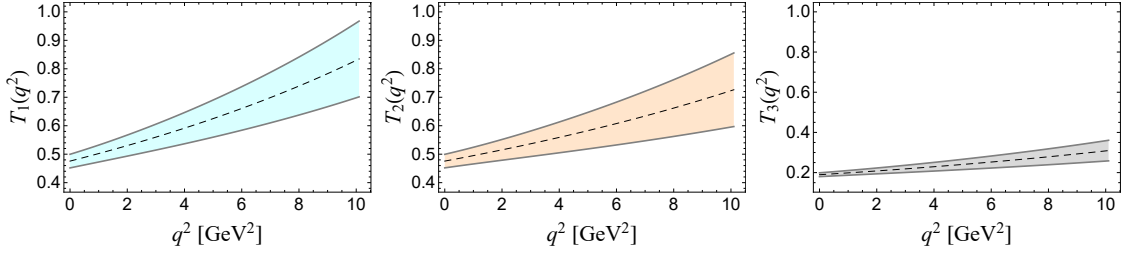

Figure 3: Tensor form factors for $B_c \to J/\psi$ calculated in this paper.

by q, the momentum carried by the lepton pair system), so that

$$p_{B_c\mu} = m_{B_c}v_\mu; \quad (p_{\eta_c, J/\psi})_\mu = m_{\eta_c, J/\psi}v_\mu + q'_\mu. \tag{2.45}$$

The parameter a_0 is connected to the Bohr radius of the B_c meson, it value is not important for the further discussion and will not be discussed here.

We can now relate the $\Delta(a_0 q')$ function to the $B_c \to \eta_c$ form factor $f_+(q^2)$ at the zero recoil as

$$\Delta(a_0 q') \approx \sqrt{\frac{m_{B_c}}{m_{\eta_c}}} f_+(q^2_{\max}), \tag{2.46}$$

which amounts, using the predicted $f_+(q^2_{\max})$ from the calculation above, to

$$\Delta(a_0 q')_{\text{our}} \approx 0.79 \pm 0.09. \tag{2.47}$$

This value can be compared with the value obtained in the QCD relativistic potential model in [86].

In [85] it was shown that in the NRQCD approximation one can derive a generalized set of relations using the HQSS, so that the transition form factors of $B_c \to \eta_c$ and $B_c \to J/\psi$ decays can be given in terms of a single form factor, even for the case of non-equal four-velocities $v_1 \neq v_2$, of the initial and the final state heavy mesons. If the following helicity basis for the form factors in $B_c \to J/\psi$ decay is defined

$$g(q^2) \equiv (H_{++} - H_{--})/\sqrt{\lambda(m_{B_c}, m_{J/\psi}, q^2)} = \frac{2}{m_{B_c} + m_{J/\psi}} V(q^2),$$

$$f(q^2) \equiv -(H_{++} + H_{--})/2 = (m_{B_c} + m_{J/\psi}) A_1(q^2),$$

$$\begin{aligned}
\mathcal{F}_1(q^2) &\equiv -\sqrt{q^2} H_{00} \\
&= \frac{1}{m_{J/\psi}} \left[-\frac{\lambda(m_{B_c}, m_{J/\psi}, q^2)}{2(m_{B_c} + m_{J/\psi})} A_2(q^2) \right. \\
&\left. \quad - \frac{1}{2}(q^2 - m_{B_c}^2 + m_{J/\psi}^2)(m_{B_c} + m_{J/\psi}) A_1(q^2) \right],
\end{aligned} \tag{2.48}$$

$$\mathcal{F}_2(q^2) \equiv -2\frac{\sqrt{q^2}}{\sqrt{\lambda(m_{B_c}^2, m_{J/\psi}^2, q^2)}} H_{t0} = 2A_0(q^2),$$

and

$$\lambda(m_{B_c}, m_{J/\psi}, q^2) = (q^2 + m_{B_c}^2 - m_{J/\psi}^2)^2 - 4m_{B_c} q^2. \tag{2.49}$$

the expressions from [85], stemming from considering NRQCD and HQSS, and relating different decay form factors at the point of zero recoil $q_{\max}^2$ of $\bar{Q}q \to \bar{Q}'q$ transitions can be expressed as [22]:

$$g(q_{\max}^2) = \frac{3 + r_Q}{4m_{B_c}^2 r_{J/\psi}} f(q_{\max}^2),$$

$$\mathcal{F}_1(q_{\max}^2) = m_{B_c}(1 - r_{J/\psi}) f(q_{\max}^2), \tag{2.50}$$

$$\mathcal{F}_2(q_{\max}^2) = \frac{2(1 + r_{J/\psi}) + (1 - r_{J/\psi})(1 - r_Q)}{4m_{B_c} r_{J/\psi}} f(q_{\max}^2),$$

for the $B_c \to J/\psi$ decay, and

$$f_0(q_{\max}^2) = \frac{1}{m_{B_c}^2 - m_{\eta_c}^2} \frac{8m_{B_c}^2(1 - r_{\eta_c})r_{\eta_c}}{2(1 + r_{\eta_c}) + (1 - r_{\eta_c})(1 - r_Q)} f_+(q_{\max}^2), \tag{2.51}$$

for the $B_c \to \eta_c$ decay [23], where some shorthand notation has been introduced: $r_M = m_M/m_{B_c}$ (with $m_M = [m_{J/\psi}, m_{\eta_c}]$), $r_Q = m_{Q'}/m_Q = m_c/m_b$ and $r_q = m_q/m_Q = r_Q$. Additionally, the vector decay form factors can be related to the pseudoscalar ones as [24]

$$f(q_{\max}^2) = \frac{8m_{B_c} r_{\eta_c}}{3 + r_{\eta_c} - (1 - r_{\eta_c})r_Q} f_+(q_{\max}^2),$$

$$g(q_{\max}^2) = \frac{1 + r_Q}{m_{B_c} r_{J/\psi}} \frac{4r_{\eta_c}}{3 + r_{\eta_c} - (1 - r_{\eta_c})r_Q} f_+(q_{\max}^2),$$

$$\mathcal{F}_1(q_{\max}^2) = m_{B_c}^2(1 - r_{J/\psi}) \frac{8r_{\eta_c}}{3 + r_{\eta_c} - (1 - r_{\eta_c})r_Q} f_+(q_{\max}^2), \tag{2.52}$$

$$\mathcal{F}_2(q_{\max}^2) = \frac{1 + r_{J/\psi}}{r_{J/\psi}} \frac{4r_{\eta_c}}{3 + r_{\eta_c} - (1 - r_{\eta_c})r_Q} f_+(q_{\max}^2),$$

where we have used that $r_q = r_Q$ for $B_c \to \eta_c, J/\psi$ and simplified the relations. It is expected that these relations are broken by terms of order $\mathcal{O}(m_c/m_b, \Lambda_{\text{QCD}}/m_c) \lesssim 30\%$.

Here we check the consistency of these relations and our form factor results. At the zero-recoil $\mathcal{F}_1(q^2)$ and $f(q^2)$ are the same up to a constant factor, Eq. (2.50), which explicitly gives

$$\frac{\mathcal{F}_1(q^2_{\max})}{f(q^2_{\max})} = m_{B_c}(1 - r_{J/\psi}) = 3.18, \tag{2.53}$$

whereas

$$\frac{g(q^2_{\max})|}{g(q^2_{\max})|_{\text{Eq.(2.50)}}} \approx 0.81,$$

$$\frac{\mathcal{F}_2(q^2_{\max})|}{\mathcal{F}_2(q^2_{\max})|_{\text{Eq.(2.50)}}} \approx 0.89, \tag{2.54}$$

and

$$\frac{f_0(q^2_{\max})|}{f_0(q^2_{\max})|_{\text{Eq.(2.51)}}} \approx 1.18. \tag{2.55}$$

We see that the HQSS/NRQCD predictions are quite consistent with our sum rule predictions for the form factors at the zero recoil and can be safely used in model-independent bounds on R ratios as it was done in [22–24], keeping in mind that their accuracy is limited to $\mathcal{O}(30\%)$. Finally, using Eq. (2.52) we obtain,

$$\frac{f(q^2_{\max})|}{f(q^2_{\max})|_{\text{Eq.(2.52)}}} \approx 1.02,$$

$$\frac{g(q^2_{\max})|}{g(q^2_{\max})|_{\text{Eq.(2.52)}}} \approx 1.05,$$

$$\frac{\mathcal{F}_1(q^2_{\max})|}{\mathcal{F}_1(q^2_{\max})|_{\text{Eq.(2.52)}}} \approx 1.02, \tag{2.56}$$

$$\frac{\mathcal{F}_2(q^2_{\max})|}{\mathcal{F}_2(q^2_{\max})|_{\text{Eq.(2.52)}}} \approx 1.02,$$

an excellent agreement among the relations between $B_c \to \eta_c$ and $B_c \to J/\psi$ transition form factors derived from HQSS/NRQCD symmetry relations and our exact results at the zero recoil.

3 R_{η_c}, $R_{J/\psi}$ and decay distributions of $B_c \to \eta_c \ell \nu_\ell$ and $B_c \to J/\psi \ell \nu_\ell$

The general effective Lagrangian for the quark level transition $b \to c \ell \nu_\ell$ with $\ell = e, \mu, \tau$ is given by

$$\mathcal{L} = \frac{G_F V_{cb}}{\sqrt{2}} \left[(1 + V_L)\mathcal{O}_{V_L} + V_R \mathcal{O}_{V_R} + S_L \mathcal{O}_{S_L} + S_R \mathcal{O}_{S_R} + T_L \mathcal{O}_{T_L}\right], \tag{3.1}$$

with the four-Fermi operators defined as

$$\mathcal{O}_{V_L} = (\bar{c}\gamma^\mu(1 - \gamma_5)b)\left(\bar{\ell}\gamma_\mu(1 - \gamma_5)\nu_\ell\right), \quad \mathcal{O}_{V_R} = (\bar{c}\gamma^\mu(1 + \gamma_5)b)\left(\bar{\ell}\gamma_\mu(1 - \gamma_5)\nu_\ell\right),$$

$$\mathcal{O}_{S_L} = (\bar{c}(1 - \gamma_5)b)\left(\bar{\ell}(1 - \gamma_5)\nu_\ell\right), \quad \mathcal{O}_{S_R} = (\bar{c}(1 + \gamma_5)b)\left(\bar{\ell}(1 - \gamma_5)\nu_\ell\right),$$

$$\mathcal{O}_{T_L} = (\bar{c}\sigma^{\mu\nu}(1 - \gamma_5)b)\left(\bar{\ell}\sigma_{\mu\nu}(1 - \gamma_5)\nu_\ell\right). \tag{3.2}$$

We use $\sigma_{\mu\nu} = i\left[\gamma_\mu, \gamma_\nu\right]/2$ and $V_{L,R}, S_{L,R}, T_L$ are the complex Wilson coefficients governing the NP contributions which are zero in the SM. Since we want to explain the possible lepton-flavour non-universality, we will assume that the NP effects contribute to the τ leptons only. The matrix element of the semileptonic decays $B_c \to J/\psi(\eta_c)\tau\nu_\tau$ then has the form:

$$\mathcal{M} = \frac{G_F V_{cb}}{\sqrt{2}} \left[\left\{(1 + V_L + V_R)\langle J/\psi(\eta_c)| \bar{c}\gamma^\mu b |\bar{B}_c\rangle + (V_R - V_L)\langle J/\psi(\eta_c)| \bar{c}\gamma^\mu\gamma_5 b |\bar{B}_c\rangle\right\}\bar{\ell}\gamma_\mu(1 - \gamma_5)\nu_\ell\right.$$

$$+ (S_R + S_L)\langle J/\psi(\eta_c)| \bar{c}b |\bar{B}_c\rangle \bar{\ell}(1 - \gamma_5)\nu_\ell + (S_R - S_L)\langle J/\psi(\eta_c)| \bar{c}\gamma_5 b |\bar{B}_c\rangle \bar{\ell}(1 - \gamma_5)\nu_\ell$$

$$\left. + T_L \langle J/\psi(\eta_c)| \bar{c}\sigma^{\mu\nu}(1 - \gamma_5)b |\bar{B}_c\rangle \bar{\ell}\sigma^{\mu\nu}(1 - \gamma_5)\nu_\ell\right]. \tag{3.3}$$

We note that the axial and the pseudoscalar hadronic currents do not contribute to the $B_c \to \eta_c$ decay, and therefore $V_R - V_L = 0, S_R - S_L = 0, \Rightarrow V_R = V_L, S_R = S_L$. The scalar hadronic current does not contribute to the $B_c \to J/\psi$ transition which leads to $S_L + S_R = 0$. We henceforth use the shorthand definition $S_R + S_L = S$ and $S_R - S_L = P$ in the text.

The constraints on the Wilson coefficients appearing in Eq. (3.1) are obtained from the combined analysis of the BaBar, Belle and LHCb data for the branching fraction ratios $R_{D^{(*)}}$, the τ polarization asymmetry along the longitudinal directions of the τ lepton in $B \to D^*$, as well as the longitudinal D^* polarization in $B_c \to D^* \tau \nu_\tau$ decay [43]. The leptonic branching fraction of the B_c meson, $BR(B_c \to \tau\nu)$, is not yet measured, therefore the possible NP contributions come from precise experimental measurements of the B_c lifetime, $\tau_{B_c}^{\mathrm{exp}} = (0.507 \pm 0.009)$ ps [87]. The theoretical SM prediction of the B_c lifetime still allows for up to 60% contribution from NP [43, 88] in the B_c leptonic decay width. In particular, the best fit point for S_R is dependent on the assumption of the $B_c \to \tau\nu$ decay width.

We consider for our analysis the limit $\mathrm{BR}(B_c \to \tau\bar\nu) < 30\%$ and the values of the Wilson coefficients from the combined analysis done in Ref. [43]. They studied all one-dimensional scenarios with only one NP Wilson coefficient considered at a time and the two-dimensional scenarios with two NP Wilson coefficients considered simultaneously. The best fit points in the 1D scenarios and their 2σ ranges (given in square brackets below) at 1 TeV are given in Table 1 of Ref. [43] and we list them below for completion:

$$\begin{aligned}
&V_L = 0.11 \; [0.06, \; 0.15], \\
&S_R = 0.16 \; [0.08, \; 0.23], \quad S_L = 0.12 \; [0.01, \; 0.20], \\
&S_L = 4T_L = -0.07 \; [-0.15, \; 0.02].
\end{aligned} \tag{3.4}$$

Only the real values of the coefficients were considered for the fit. The possibility of allowing imaginary coefficients was examined in Ref. [89] and they obtained that the relation $\mathrm{Im}[S_L] = 4\,\mathrm{Im}[T_L]$ is also permitted by the recent experiments. We therefore use the best fit value for $S_L = 4T_L$ in Eq. (3.4) for both, the real and the imaginary case. The results of the fit for the NP Wilson coefficients in the 2D scenario at 1 TeV are taken from Table 2 of Ref. [43]:

$$\begin{aligned}
&(V_L, \; S_L) = -4T_L = (0.08, \; 0.05), \\
&(S_R, \; S_L) = (-0.30, \; -0.64), \\
&(V_L, \; S_R) = (0.09 \; 0.06), \\
&(\mathrm{Re}[S_L = 4\,T_L], \mathrm{Im}[S_L = 4\,T_L]) = (-0.06, \pm 0.40).
\end{aligned} \tag{3.5}$$

All NP operators are generated by the addition of a single new particle to the SM. The relation $S_L = 4T_L$ is generated in the R_2 leptoquark scenario with a scalar $SU(2)_L$ doublet [90, 91] at the new physics scale. The leptoquark model with an $SU(2)_L$ singlet scalar S_1 gives the relation $S_L = -4T_L$ at the NP scale. These relations are modified at the scale m_b to: $S_L(m_b) \simeq 8.1 T_L(m_b)$ for R_2, and $S_L(m_b) \simeq -8.5 T_L(m_b)$, after including one-loop electroweak corrections in addition to the three-loop QCD anomalous dimensions in the renormalization group running using the following relations [92]:

$$\begin{aligned}
&V_L(m_b) = V_L(1 \text{ TeV}), \quad S_R(m_b) = 1.737 S_R(1 \text{ TeV}), \\
&\begin{pmatrix} S_L(m_b) \\ T_L(m_b) \end{pmatrix} = \begin{pmatrix} 1.752 & -0.287 \\ -0.004 & 0.842 \end{pmatrix} \begin{pmatrix} S_L(1 \text{ TeV}) \\ T_L(1 \text{ TeV}) \end{pmatrix}.
\end{aligned} \tag{3.6}$$

We now discuss the differential decay rates for the processes $B_c \to \eta_c \ell \nu_\ell$ and $B_c \to J/\psi \ell \nu_\ell$. The differential decay rate for these semi-leptonic processes depend on the angle θ_ℓ which is the

polar angle of the lepton ℓ (the angle between the lepton direction in the W^* rest frame and the direction of the W^* in the B_c rest frame) and the momentum transfer q^2 ($q = p_{B_c} - p$) to the $\ell\nu_\ell$ pair. The differential $(q^2, \cos\theta_\ell)$ distribution can be calculated using the helicity techniques and is of the form

$$\frac{d^2\Gamma}{dq^2 d\cos\theta_\ell} = \frac{G_F^2 |V_{cb}|^2 |\mathbf{p_2}| v}{(2\pi)^3 64 m_{B_c}^2} H_{\mu\nu} L^{\mu\nu}(\theta_\ell), \tag{3.7}$$

where $|\mathbf{p_2}| = \lambda^{1/2}(m_{B_c}^2, m_{\eta_c, J/\psi}^2, q^2)/2m_{B_c}$ is the momentum of $\eta_c(J/\psi)$ in the B_c rest frame, $v = (1 - m_\ell^2/q^2)$ is the lepton velocity in the $\ell^- \bar\nu_\ell$ center-of-mass frame and $H_{\mu\nu} L^{\mu\nu}$ is the contraction of the hadronic and the leptonic tensors. The helicity techniques to calculate the angular distribution in the presence of new physics operators for the semi-leptonic decays considered here can be found in Ref. [93, 94].

The differential distribution for the $B_c \to \eta_c \tau \nu_\tau$ is written as

$$\begin{aligned}
\frac{d^2\Gamma(\eta_c)}{dq^2 d\cos\theta_\ell} &= \frac{G_F^2 |V_{cb}|^2 |\mathbf{p_2}| q^2 v^2}{(2\pi)^3 16 m_{B_c}^2} \Big\{ |1 + V_L + V_R|^2 \left[|H_0|^2 \sin^2\theta_\ell + 2\delta_\ell |H_t - H_0 \cos\theta_\ell|^2 \right] \\
&+ |S|^2 |H_P^S|^2 + 16|T_L|^2 \left[2\delta_\ell + (1 - 2\delta_\ell)\cos^2\theta_\ell \right] |H_T|^2 \\
&+ 2\sqrt{2\delta_\ell}\Big(\mathrm{Re}S + S\,V_L \Big) H_P^S [H_t - H_0 \cos\theta_\ell] \\
&+ 8\sqrt{2\delta_\ell}\Big(\mathrm{Re}T_L + T_L V_L \Big) [H_0 - H_t \cos\theta_\ell] H_T - 8H_P^S H_T \cos\theta_\ell \Big(T_L S \Big) \Big\}, \tag{3.8}
\end{aligned}$$

with the helicity flip-factor $\delta_\ell = m_\ell^2/2q^2$, $T_L V_L = \mathrm{Re}T_L\,\mathrm{Re}V_L + \mathrm{Im}T_L\,\mathrm{Im}V_L$, $T_L S = \mathrm{Re}T_L\,\mathrm{Re}S + \mathrm{Im}T_L\,\mathrm{Im}S$ and $S\,V_L = \mathrm{Re}S\,\mathrm{Re}V_L + \mathrm{Im}S\,\mathrm{Im}V_L$. We consider the interference between the different NP operators as their effect can be similar to NP^2, if they are of the same value. The $H's$ in Eq. (3.8) are the hadronic helicity amplitudes written in terms of the invariant form factors defined in Eq. (2.1) and are of the form

$$H_t = \frac{Pq}{\sqrt{q^2}} f_0, \quad H_0 = \frac{2m_{B_c}|\mathbf{p_2}|}{\sqrt{q^2}} f_+, \quad H_P^S = \frac{Pq}{m_b(\mu) - m_c(\mu)} f_0, \quad H_T = \frac{2m_{B_c}|\mathbf{p_2}|}{m_{B_c} + m_{\eta_c}} f_T, \tag{3.9}$$

with $P = p_{B_c} + p$ and $q = p_{B_c} - p$ ($p = p_{\eta_c}$ or $p = p_{J/\psi}$).

Next, the differential distribution of the $\bar{B}_c \to J/\psi \ell^- \bar\nu_\ell$ decay is considered with $V_R V_L = \mathrm{Re}V_R\,\mathrm{Re}V_L + \mathrm{Im}V_R\,\mathrm{Im}V_L$, $T_L P = \mathrm{Re}T_L\,\mathrm{Re}P + \mathrm{Im}T_L\,\mathrm{Im}P$ and $P V_L = \mathrm{Re}P\,\mathrm{Re}V_L + \mathrm{Im}P\,\mathrm{Im}V_L$, and is given by

$$\begin{aligned}
\frac{d^2\Gamma(J/\psi)}{dq^2 d\cos\theta_\ell} &= \frac{G_F^2 |V_{cb}|^2 |\mathbf{p_2}| q^2 v^2}{32(2\pi)^3 m_{B_c}^2} \Big\{ |1 + V_L|^2 \Big[(1 - \cos\theta_\ell)^2 |H_{++}|^2 + (1 + \cos\theta_\ell)^2 |H_{--}|^2 + 2\sin^2\theta_\ell |H_{00}|^2 \\
&+ 2\delta_\ell \Big(\sin^2\theta_\ell (|H_{++}|^2 + |H_{--}|^2) + 2|H_{t0} - H_{00}\cos\theta_\ell|^2 \Big) \Big] \\
&+ |V_R|^2 \Big[(1 - \cos\theta_\ell)^2 |H_{--}|^2 + (1 + \cos\theta_\ell)^2 |H_{++}|^2 + 2\sin^2\theta_\ell |H_{00}|^2 \\
&+ 2\delta_\ell \Big(\sin^2\theta_\ell (|H_{++}|^2 + |H_{--}|^2) + 2|H_{t0} - H_{00}\cos\theta_\ell|^2 \Big) \Big] - 4\Big(\mathrm{Re}V_R + V_R V_L \Big) \\
&\quad \Big[(1 + \cos^2\theta_\ell) H_{++} H_{--} + \sin^2\theta_\ell |H_{00}|^2 + 2\delta_\ell \Big(\sin^2\theta_\ell H_{++}H_{--} + |H_{t0} - H_{00}\cos\theta_\ell|^2 \Big) \Big] \\
&+ 2|P|^2 |H_V^S|^2 + 4\sqrt{2\delta_\ell} H_V^S (H_{t0} - H_{00}\cos\theta_\ell)\Big(\mathrm{Re}P + P V_L \Big) + 16\cos\theta_\ell H_V^S H_T^0 T_L P \\
&+ 16|T_L|^2 \Big[|H_T^0|^2 \Big(1 + 2\delta_\ell + (1 - 2\delta_\ell)\cos 2\theta_\ell \Big) + 2|H_T^+|^2 \sin^2\frac{\theta_\ell}{2}\Big(1 + 2\delta_\ell + (1 - 2\delta_\ell)\cos\theta_\ell \Big) \\
&+ 2|H_T^-|^2 \cos^2\frac{\theta_\ell}{2}\Big(1 + 2\delta_\ell - (1 - 2\delta_\ell)\cos\theta_\ell \Big) \Big] - 16\sqrt{2\delta_\ell}\Big(\mathrm{Re}T_L + T_L V_L \Big) \\
&\quad \Big[H_{++}H_T^+ + H_{--}H_T^- + H_{00}H_T^0 - \Big(H_{++}H_T^+ - H_{--}H_T^- + H_{t0}H_T^0 \Big)\cos\theta_\ell \Big] \Big\}. \tag{3.10}
\end{aligned}$$

The hadronic helicity amplitudes in terms of the form factors given in Eqs. (2.3, 2.7) are expressed as

$$
H_{\pm\pm} = \frac{-(m_{B_c} + m_{J/\psi})^2 A_1 \pm 2m_{B_c}|\mathbf{p_2}|V}{m_{B_c} + m_{J/\psi}}, \quad H_V^S = \frac{2m_{B_c}}{m_b(\mu) + m_c(\mu)}|\mathbf{p_2}|A_0,
$$

$$
H_{00} = \frac{-(m_{B_c}^2 - m_{J/\psi}^2 - q^2)(m_{B_c} + m_{J/\psi})^2 A_1 + 4m_{B_c}^2|\mathbf{p_2}|^2 A_2}{2m_{J/\psi}\sqrt{q^2}(m_{B_c} + m_{J/\psi})}, H_{t0} = -\frac{2m_{B_c}|\mathbf{p_2}|}{\sqrt{q^2}}A_0
$$

$$
H_T^{\pm} = -\frac{1}{\sqrt{q^2}}\left[\pm\lambda^{1/2}[m_{B_c}^2, m_{J/\psi}^2, q^2]T_1 + (m_{B_c}^2 - m_{J/\psi}^2)T_2\right],
$$

$$
H_T^0 = = -\frac{1}{2m_{J/\psi}}\left[(m_{B_c}^2 + 3m_{J/\psi}^2 - q^2)T_2 - \frac{\lambda[m_{B_c}^2, m_{J/\psi}^2, q^2]}{m_{B_c}^2 - m_{J/\psi}^2}T_3\right]. \tag{3.11}
$$

3.1 Results for the branching ratios and $R_{\eta_c}, R_{J/\psi}$ predictions

We first give our predictions for branching fractions in the SM of both decays in Table 3, where we put the branching fraction values updated using the latest value for the B_c lifetime, $\tau_{B_c} = (0.507 \pm 0.009)$ ps [87], while in the brackets we cite the original published values of the BRs. If there are no brackets the branching fractions have already been calculated using the latest value for τ_{B_c}.

Mode	this work	QCDSR [3]	SR [5]	pQCD [2]	RCQM [14]	CCQM [25, 77]	RQM [9]	RQM [6]	RQM [8]	RQM [7]	LFQM [12]
$B_c \to \eta_c l\bar{\nu}_l$	$0.82^{+0.12}_{-0.11}$	0.85 (0.75)	1.85 (1.64)	0.50 (0.44)	0.91 (0.81)	0.95	0.47 (0.42)	0.89	0.52 (0.52)	0.85	0.74 (0.67)
$B_c \to \eta_c \tau\bar{\nu}_\tau$	$0.26^{+0.06}_{-0.05}$	0.25 (0.23)	0.55 (0.49)	0.15 (0.14)	0.25 (0.22)	0.24	-	-	-	-	0.21 (0.19)
$B_c \to J/\psi l\bar{\nu}_l$	$2.24^{+0.57}_{-0.49}$	2.16 (1.9)	2.67 (2.37)	1.13 (1.00)	2.33 (2.07)	1.67	1.39 (1.23)	1.42	1.49 (1.47)	2.33	1.64 (1.49)
$B_c \to J/\psi \tau\bar{\nu}_\tau$	$0.53^{+0.16}_{-0.14}$	0.54 (0.48)	0.73 (0.65)	0.33 (0.29)	0.55 (0.49)	0.40	-	-	-	-	0.41 (0.37)

Table 3: Branching fractions of $B_c \to J/\psi, \eta_c$ decays calculated in different models and given in %, with l denoting a light lepton, e or μ.

The ratios of semileptonic branching fractions using our calculated form factors from Eq. (2.39) are

$$
R_{\eta_c}|_{\rm SM} \equiv \frac{\Gamma(B_c \to \eta_c\tau\bar{\nu}_\tau)}{\Gamma(B_c \to \eta_c\mu\bar{\nu}_\mu)} = 0.32 \pm 0.02, \tag{3.12}
$$

$$
R_{J/\psi}|_{\rm SM} \equiv \frac{\Gamma(B_c \to J/\psi\tau\bar{\nu}_\tau)}{\Gamma(B_c \to J/\psi\mu\bar{\nu}_\mu)} = 0.23 \pm 0.01. \tag{3.13}
$$

We see that above results agree with the recent model-independent analysis of $R_{J/\psi}$ [22, 24] and R_{η_c} [23, 24]. See also the discussion in Sec.2.2.1.

The ratios of the branching fractions $R_{J/\psi,\eta_c}$ are computed next in the context of different NP scenarios using the form factors calculated in Sec. 2. The values of the NP operators' effective couplings considered for our analysis are discussed before and are given by Eqs. (3.4, 3.5). In Fig. 4 we show the the q^2 dependence of the ratios R_{η_c} and $R_{J/\psi}$ in the presence of only one NP operator (first two figures of both panels). The third figure in both panels shows the ratio in presence of two NP operators. The SM value is always shown by the blue dotted line. We see that the ratio increases for most of NP contributions for both J/ψ and η_c. The $S_L = 4T_L$ case with the coupling

being pure real or imaginary results in a decrease in the ratio R_{η_c}. This is due to the negative interference between S_L and T_L, Eq. (3.8). The shaded region shows the 2σ allowed region for $V_L, S_L = 4T_L, S_{L,R}$ parameters in the 1D fit, with the central value shown by a dashed line. In case of the 2D scenarios the results are presented for the best fit point. As expected, the ratio R_{η_c} is more sensitive to the scalar and the tensor operators, whereas $R_{J/\psi}$ is more sensitive to V_L. The
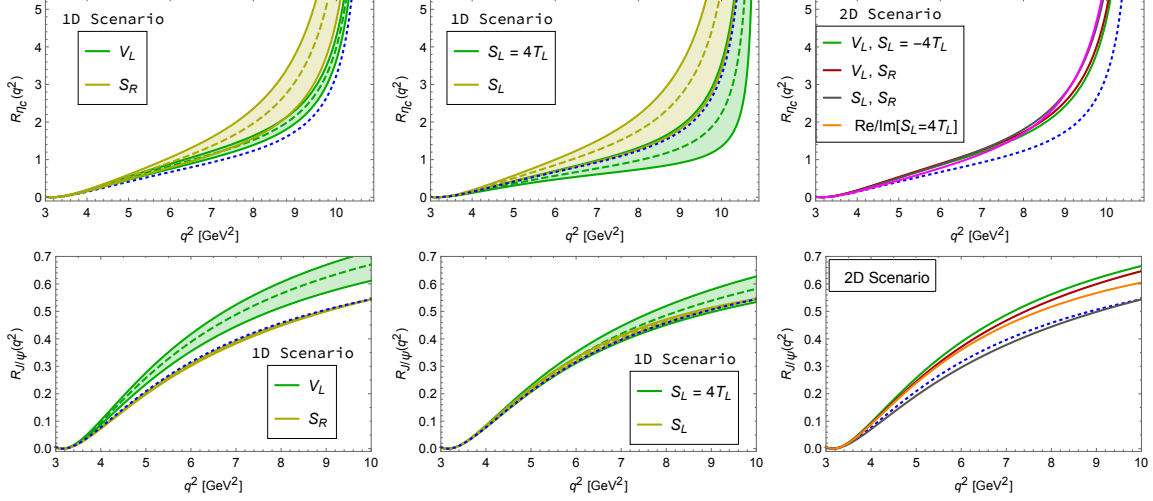

Figure 4: Ratios of branching fractions $R_{\eta_c}(q^2)$ (upper panel), $R_{J/\psi}(q^2)$ (lower panel) as a function of q^2. The blue dotted lines are the SM prediction, the green dashed line is for the best fit values of the NP couplings in the 1D scenario as discussed in the text. The green band represents the NP effects from the 2σ allowed regions in the 1D scenarios. The third figure in both panels is the result for the best fit points in the 2D scenarios.

values of $R_{J/\psi}$ and R_{η_c} in the presence of different NP scenarios are listed in Table 4. The results are presented for the best fit points, as well as for the 2σ allowed regions in the 1D scenario.

Note that any of the considered NP scenarios derived from the recent global fit analysis on available experimental data on semileptonic $B \to (D, D^*)\ell\nu_\ell$ decays [43] cannot explain the 2σ tension with the experiment Eq. 1.1 of $R_{J/\psi}$ ratio.

	SM	V_L	S_L	S_R	$S_L = 4T_L$	$(V_L, S_L = -4T_L)$	(S_R, S_L)	(V_L, S_R)	Re,Im$[S_L = 4T_L]$
R_{η_c}	0.32	$0.39^{0.42}_{0.36}$	$0.44^{0.55}_{0.33}$	$0.49^{0.59}_{0.40}$	$0.26^{0.34}_{0.20}$	0.42	0.45	0.44	0.43
$R_{J/\psi}$	0.23	$0.29^{0.31}_{0.26}$	$0.24^{0.24}_{0.23}$	$0.23^{0.22}_{0.23}$	$0.25^{0.26}_{0.23}$	0.29	0.22	0.27	0.26

Table 4: The values of R_{η_c} and $R_{J/\psi}$ in the presence of different NP scenarios. The subscript and the superscript are the values for the 2σ range of the NP couplings.

3.2 Forward-backward asymmetry, convexity parameter and the τ polarization

The differential distributions defined in Eqs. (3.8, 3.10) can be written in a simple form as a function of $\cos\theta_\ell$ as

$$\frac{d\Gamma}{dq^2 d\cos\theta_\ell} = \frac{G_F^2 |V_{cb}|^2 |\mathbf{p_2}| q^2 v^2}{32(2\pi)^3 m_{B_c}^2} (\mathcal{A}(q^2) + \mathcal{B}(q^2)\cos\theta_\ell + \mathcal{C}(q^2)\cos^2\theta_\ell). \quad (3.14)$$

Observables depending on the polar angle distribution of the emitted leptons such as the forward-backward lepton asymmetry and the convexity parameter are considered first. They are defined

by

$$A^{FB}(q^2) = \frac{\left(\int_0^1 - \int_{-1}^0\right) d\cos\theta_\ell \frac{d^2\Gamma}{dq^2 d\cos\theta_\ell}}{\left(\int_0^1 + \int_1^0\right) d\cos\theta_\ell \frac{d^2\Gamma}{dq^2 d\cos\theta_\ell}} = \frac{\mathcal{B}(q^2)}{2\left(\mathcal{A}(q^2) + \mathcal{C}(q^2)/3\right)},$$

$$C_F^\tau(q^2) = \frac{1}{d\Gamma/dq^2} \frac{d^2(d\Gamma/dq^2)}{d(\cos\theta_\ell)^2} = \frac{\mathcal{C}(q^2)}{\left(\mathcal{A}(q^2) + \mathcal{C}(q^2)/3\right)}. \tag{3.15}$$

The $\mathcal{A}(q^2), \mathcal{B}(q^2)$ and $\mathcal{C}(q^2)$ functions can be easily obtained from Eqs. (3.8, 3.10). We present in Figs. 5, 6 the q^2 dependence of the forward-backward asymmetry $A_{FB}(q^2)$ and the convexity parameter $C_F^\tau(q^2)$. These observables are not sensitive to the case where V_L is the only NP contribution. The $B_c \to \eta_c$ transition appears to be more sensitive to the new physics operators as compared to the $B_c \to J/\psi$ transition. In case of the J/ψ decay mode, the presence of the S_L, S_R coefficients in the 2D scenario leads to a significant deviation from $A^{FB}(q^2)$ prediction in the SM. The present allowed values of the coupling have a very small effect on $C_F^\tau(q^2)$ in case of J/ψ, whereas in case of η_c the $S_L = 4\,T_L$ case enhances $C_F^\tau(q^2)$ only at large values of q^2.
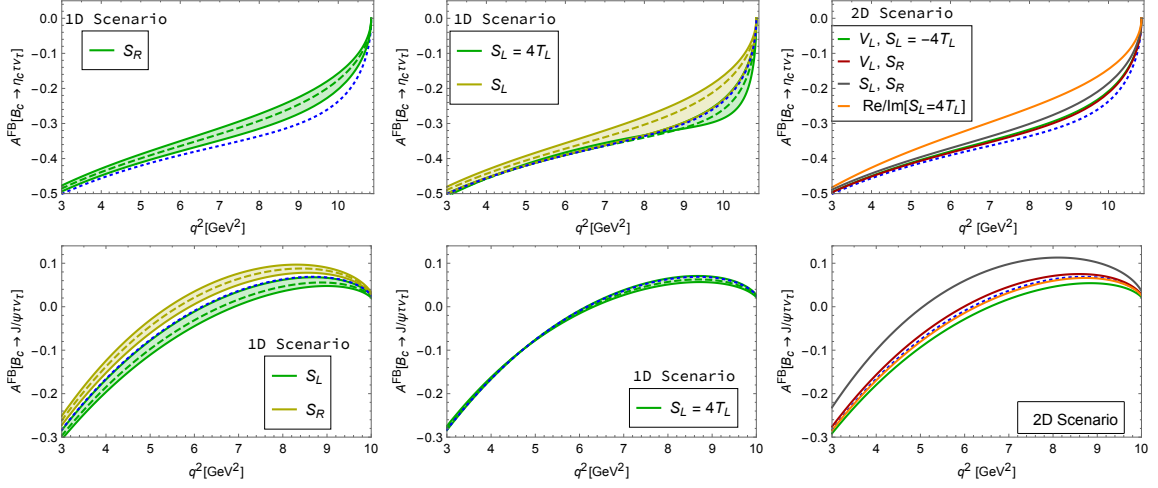

Figure 5: Forward-backward asymmetry $A^{FB}(q^2)$ for η_c (upper panel), and J/ψ (lower panel) as a function of q^2. The blue dotted lines are the SM prediction, the green dashed line is for the best fit values of the NP couplings in the 1D scenario as discussed in the text. The green band represents the NP effects from the 2σ allowed regions. The third figure in both panels is the result for the best fit points in the 2D scenarios.

Now we discuss the effect on the polarization of the emitted τ in the W^- rest frame in the presence of the NP operators. The differential decay rate for a given spin projection in a given direction can be easily obtained with the inclusion of the spin projection operators $(1 + \gamma_5 \slashed{s}_i)/2$ for τ in the calculation. The longitudinal and the transverse polarization components of the τ are then defined as:

$$P_{L,T}(q^2) = \frac{d\Gamma(s_i^\mu)/dq^2 - d\Gamma(-s_i^\mu)/dq^2}{d\Gamma(s_i^\mu)/dq^2 + d\Gamma(-s_i^\mu)/dq^2} = \frac{\mathcal{P}_{L,T}(q^2)}{2(\mathcal{A}(q^2) + \mathcal{C}(q^2)/3)}, \quad i = L, T, \tag{3.16}$$

where s_L^μ and s_T^μ are the longitudinal and the transverse polarization four-vectors of τ^- in the W^- rest frame and are given by [95–97]

$$s_L^\mu = \frac{1}{m_\tau}(|\vec{p}_\tau|, E_\tau \sin\theta_\tau, 0, E_\tau \cos\theta_\tau), \quad s_T^\mu = (0, \cos\theta_\tau, 0, -\sin\theta_\tau). \tag{3.17}$$
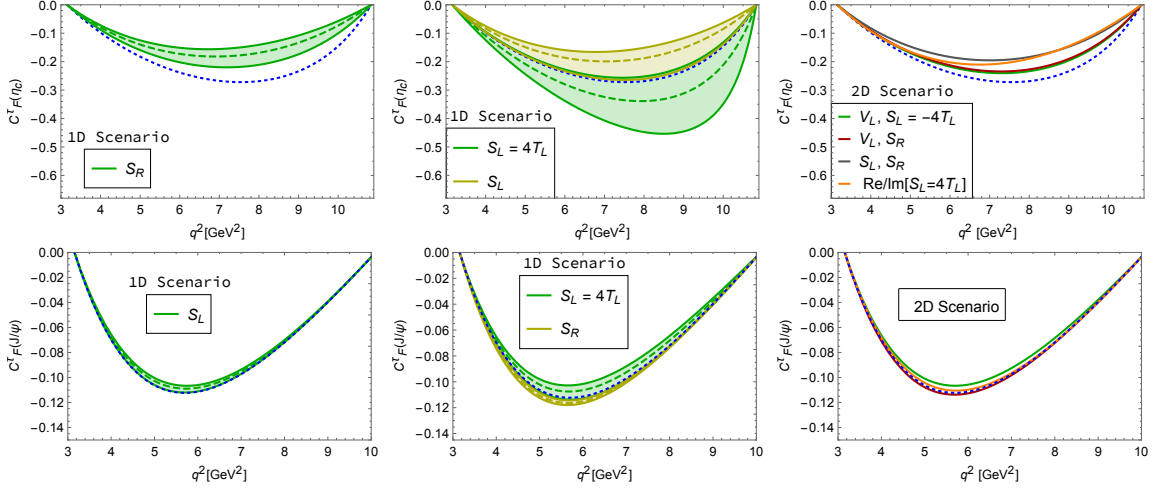
Figure 6: Convexity parameter $C_F^\tau(q^2)$ for η_c (upper panel), and J/ψ (lower panel) as a function of q^2. The blue dotted lines are the SM prediction, the green dashed line is for the best fit values of the NP couplings in the 1D scenario as discussed in the text. The green band represents the NP effects from the 2σ allowed regions. The third figure in both panels is the result for the best fit points in the 2D scenarios.

The longitudinal and transverse polarizations in the $B_c \to \eta, J/\psi \tau \nu_\tau$ decays are given as :

$$\mathcal{P}_L^{\eta_c}(q^2) = \left\{ |1 + V_L + V_R|^2 \left[-|H_0|^2 + \delta_\tau(|H_0|^2 + 3|H_t|^2) \right] + 3\sqrt{2\delta_\tau} H_P^S H_t \left(\mathrm{Re}S + S\,V_L \right) \right.$$
$$\left. + \frac{3}{2}|S|^2 |H_P^S|^2 + 8|T_L|^2(1 - 4\delta_\tau)|H_T|^2 - 4\sqrt{2\delta_\tau}\left(\mathrm{Re}T_L + T_L V_L \right) H_0 H_T \right\}, \qquad (3.18)$$

$$\mathcal{P}_L^{J/\psi}(q^2) = \left\{ (|1 + V_L|^2 + |V_R|^2)\left[-\sum_{n=\pm,0} |H_{nn}|^2 + \delta_\tau\left(\sum_{n=\pm,0} |H_{nn}|^2 + 3|H_{t0}|^2 \right) \right] + 2\mathrm{Re}V_R \right.$$

$$\left[(1 - \delta_\tau)(|H_{00}|^2 + 2H_{++}H_{--}) + 3\delta_\tau |H_{t0}|^2 \right] - 3\sqrt{2\delta_\tau}\left(\mathrm{Re}P + P\,V_L \right) H_V^S H_{t0}$$

$$\left. + \frac{3}{2}|P|^2 |H_V^S|^2 + 8|T_L|^2(1 - 4\delta_\tau)\sum_n |H_T^n|^2 + 4\sqrt{2\delta_\tau}\left(\mathrm{Re}T_L + T_L V_L \right) \sum_{n=\pm,0} H_{nn} H_T^n \right\},$$

$$\mathcal{P}_T^{\eta_c}(q^2) = \frac{3\pi\sqrt{\delta_\tau}}{2\sqrt{2}} \left\{ |1 + V_L + V_R|^2 H_0 H_t + \frac{1}{\sqrt{2\delta_\tau}}\left(\mathrm{Re}S + S\,V_L \right) H_P^S H_0 \right.$$

$$\left. + 4\sqrt{2\delta_\tau}\left(\mathrm{Re}T_L + T_L V_L \right) H_t H_T + 4H_P^S H_T T_L S \right\}, \qquad (3.19)$$

$$\mathcal{P}_T^{J/\psi}(q^2) = \frac{3\pi\sqrt{\delta_\tau}}{4\sqrt{2}} \left\{ (|1 + V_L|^2 - |V_R|^2)(|H_{--}|^2 - |H_{++}|^2) + 2(|1 + V_L|^2 + |V_R|^2)H_{t0} H_{00} \right.$$

$$- 4\mathrm{Re}V_R H_{t0} H_{00} - \frac{2}{\sqrt{2\delta_\tau}}\left(\mathrm{Re}P + P\,V_L \right) H_V^S H_{00} + 16|T_L|^2(|H_T^-|^2 - |H_T^+|^2)$$

$$\left. + 4\left(\mathrm{Re}T_L + T_L V_L \right)\left[\frac{1 + 2\delta_\tau}{\sqrt{2\delta_\tau}}(H_{++}H_T^+ - H_{--}H_T^-) - 2\sqrt{2\delta_\tau}H_{t0}H_T^0 \right] + 8H_S^V H_T^0 T_L P \right\}.$$

The transverse polarization of τ as can be seen from Eq. (3.19) has an overall factor of $\sqrt{\delta_\tau}$ and therefore vanishes in the limit of zero lepton mass and the emitted lepton is then fully longitudinally polarized. Therefore, the τ lepton can be largely transversely polarized as compared to the muons or the electrons. The q^2 dependence of the τ polarization in presence of different NP operators is shown in Figs. 7, 8. The following observations can be made from the figures. The longitudinal and transverse polarizations of τ in the η_c decay mode are more sensitive to the NP operators compared to the J/ψ decay mode. The tau transverse polarization in the J/ψ decay mode is again mostly affected by the NP operator $S_L = 4T_L$ at low values of q^2, whereas the S_L, S_R parameters in the 2D
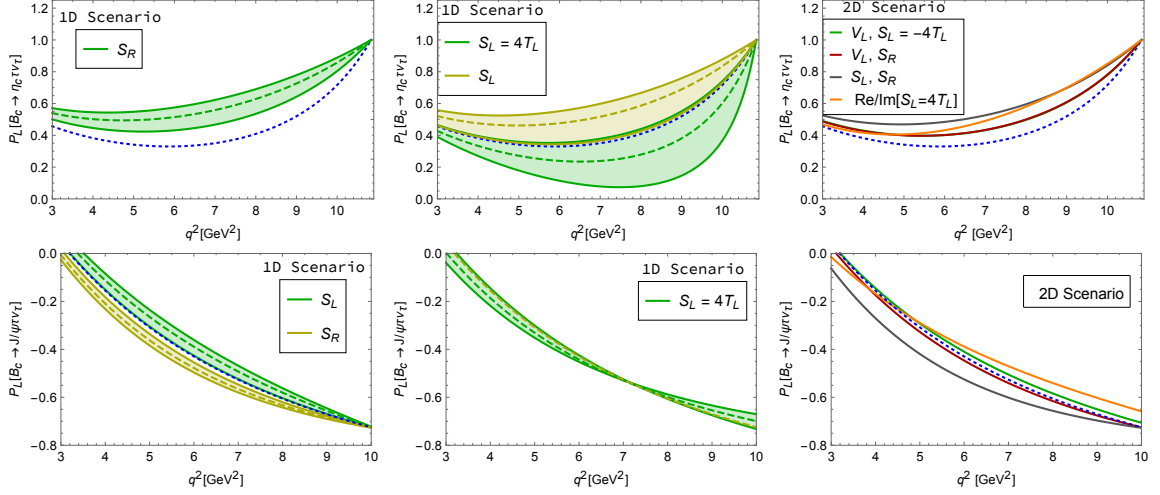
Figure 7: Longitudinal polarization of τ $(P_L^{\eta_c, J/\psi})$ in the decay of $B_c \to \eta_c \tau \nu$ (upper panel), and $B_c \to J/\psi \tau \nu_\tau$ (lower panel) as a function of q^2. The blue dotted lines are the SM prediction, the green dashed line is for the best fit values of the NP couplings in the 1D scenario as discussed in the text. The green band represents the NP effects from the 2σ allowed regions. The third figure in both panels is the result for the best fit points in the 2D scenarios.

scenario lead to a deviation from the SM prediction for both the longitudinal and the transverse τ polarization. The predictions for the mean forward-backward asymmetry, the convexity parameter and the tau polarization in the presence of different NP operators are summarised in Table 5.
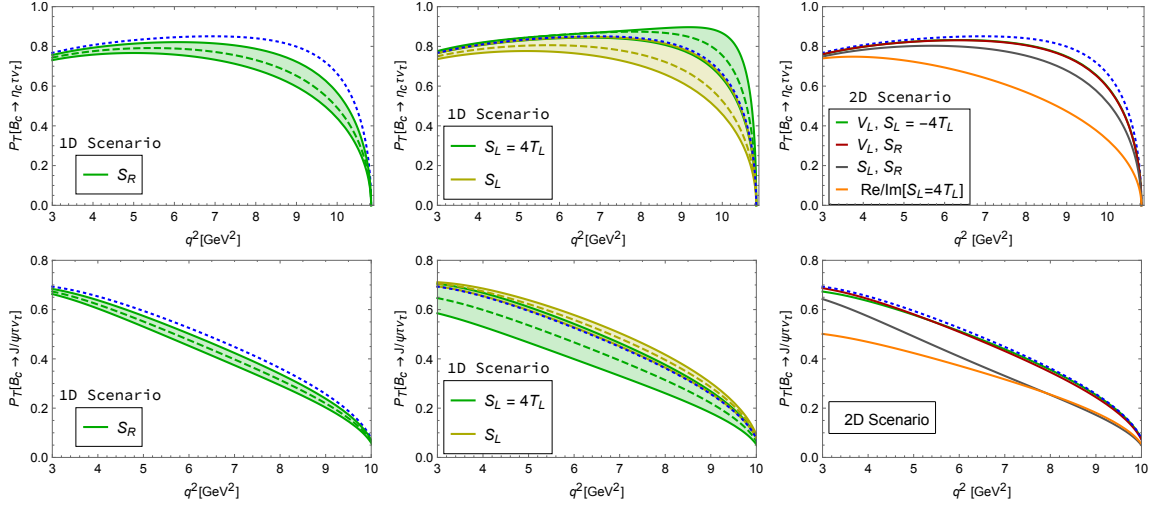

Figure 8: Transverse polarization of τ $(P_T^{\eta_c, J/\psi})$ in the decay for $B_c \to \eta_c \tau \nu$ (upper panel), and $B_c \to J/\psi \tau \nu_\tau$ (lower panel) as a function of q^2. The blue dotted lines are the SM prediction, the green dashed line is for the best fit values of the NP couplings in the 1D scenario as discussed in the text. The green band represents the NP effects from the 2σ allowed regions. The third figure in both panels is the result for the best fit points in the 2D scenarios.
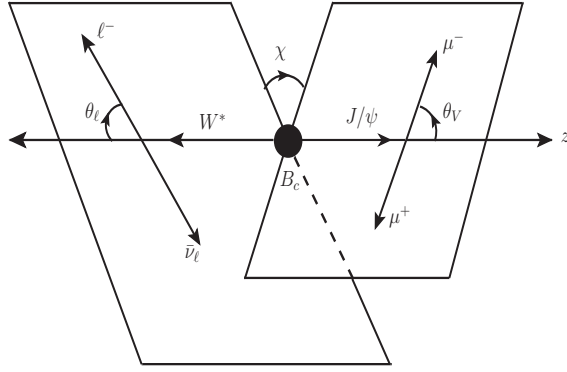
Figure 9: Angular conventions for the $B_c \to J/\psi \ell \nu_\ell$, $J/\psi \to \mu^+ \mu^-$ decay.

	SM	S_L	S_R	$S_L = 4T_L$	$(V_L, S_L = -4T_L)$	(S_R, S_L)	(V_L, S_R)	Re,Im$[S_L = 4T_L]$
$A_{FB}^{\eta_c}$	-0.35	$-0.31^{-0.29}_{-0.34}$	$-0.30^{-0.28}_{-0.32}$	$-0.36^{-0.34}_{-0.36}$	-0.33	-0.31	-0.33	-0.27
C_F^{τ,η_c}	-0.22	$-0.16^{-0.13}_{-0.21}$	$-0.14^{-0.12}_{-0.17}$	$-0.27^{-0.21}_{-0.35}$	-0.19	-0.15	-0.19	-0.16
$P_L^{\eta_c}$	0.42	$0.58^{0.66}_{0.43}$	$0.62^{0.68}_{0.53}$	$0.31^{0.45}_{0.14}$	0.50	0.59	0.50	0.57
$P_T^{\eta_c}$	0.81	$0.73^{0.80}_{0.67}$	$0.70^{0.76}_{0.66}$	$0.84^{0.86}_{0.80}$	0.77	0.72	0.77	0.43
$A_{FB}^{J/\psi}$	0.02	$0.005^{0.02}_{-0.01}$	$0.04^{0.05}_{0.03}$	$0.02^{0.02}_{0.01}$	0.006	0.07	0.03	0.02
$C_F^{\tau,J/\psi}$	-0.07	$-0.07^{-0.07}_{-0.07}$	$-0.07^{-0.07}_{-0.07}$	$-0.07^{-0.06}_{-0.07}$	-0.07	-0.08	-0.08	-0.08
$P_L^{J/\psi}$	-0.53	$-0.50^{-0.48}_{-0.53}$	$-0.57^{-0.55}_{-0.58}$	$-0.53^{-0.53}_{-0.53}$	-0.51	-0.60	-0.54	-0.48
$P_T^{J/\psi}$	0.40	$0.43^{0.45}_{0.40}$	$0.35^{0.38}_{0.33}$	$0.35^{0.41}_{0.29}$	0.39	0.29	0.38	0.28

Table 5: The integrated values of the forward-backward asymmetry, the convexity parameter and the longitudinal and transverse polarization of τ in the whole q^2 region, in case of different NP scenarios discussed in the text. The subscript and the superscript are the values for the 2σ range of the NP couplings.

4 Decay distribution of $B_c \to J/\psi \left(J/\psi \to \mu^+ \mu^- \right) \ell \nu_\ell$ decay

We consider in this section the process $B_c \to J/\psi \left(J/\psi \to \mu^+ \mu^- \right) \ell \nu_\ell$, with the 4-fold differential decay rate being dependent on three angles $\theta_V, \theta_\ell, \chi$ and the momentum transfer q^2. The angle θ_ℓ is same as defined before, θ_V is the polar angle between the direction of the emitted μ^- in the J/ψ rest frame and the parent J/ψ in the B_c rest frame, and χ is the azimuthal angle between the $W^*\ell\nu$ plane and the $J/\psi\mu^+\mu^-$ plane. The angles are shown in Fig. 9 and are defined as usually being taken in the literature. The J/ψ is too light to decay to $\tau^+\tau^-$, therefore the outgoing leptons can be either a pair of μ or of e. We ignore the mass m_μ, m_e from the J/ψ decays but the mass of lepton from W^* decay is retained. The total differential decay rate for the $\mu_L^- \mu_R^+$ ($\sigma \sim \lambda_\ell^- - \lambda_\ell^+ = -1$) final state is given by Eq. (4.1) below. The corresponding expressions for $\mu_R^- \mu_L^+$ final state can be obtained by setting $\theta_V \to \theta_V + \pi$ in Eq. 4.1.

$$\frac{d\Gamma(B_c \to J/\psi \ell \nu_\ell, J/\psi \to \mu_R^+ \mu_L^-)}{dq^2 d\cos\theta_\ell d\cos\theta_V d\chi} = \frac{3G_F^2 |V_{cb}|^2 |\mathbf{p_2}| q^2 v^2}{8(4\pi)^4 m_{B_c}^2} \text{BR}(J/\psi \to \mu_L^- \mu_R^+) \Big[|1 + V_L|^2 \mathcal{T}_{V_L} + |V_R|^2 \mathcal{T}_{|V_R|^2}$$
$$+ \mathcal{T}_{V_R^{int}} + 2|P|^2 (H_S^V)^2 \sin^2\theta_V + \mathcal{T}_{P^{int}} + |T_L|^2 \mathcal{T}_{|T_L|^2} + \mathcal{T}_{T_L^{int}} \Big], \quad (4.1)$$

with

$$\mathcal{T}_{V_L} = \sin^2\theta_V\Big(2H_{00}^2(\sin^2\theta_\ell + 2\delta_\tau\cos^2\theta_\ell) + 4\delta_\tau H_{t0}^2\Big) + 8H_{++}^2\sin^2\frac{\theta_\ell}{2}\sin^4\frac{\theta_V}{2}\Big(2\delta_\tau\cos^2\frac{\theta_\ell}{2} + \sin^2\frac{\theta_\ell}{2}\Big)$$
$$+\ 8H_{--}^2\cos^2\frac{\theta_\ell}{2}\cos^4\frac{\theta_V}{2}\Big(2\delta_\tau\sin^2\frac{\theta_\ell}{2} + \cos^2\frac{\theta_\ell}{2}\Big) + H_{++}H_{--}\sin^2\theta_\ell\sin^2\theta_V\cos 2\chi(1-2\delta_\tau)$$
$$-\ 8\sin\theta_\ell\sin\theta_V\cos\chi H_{00}\Big(H_{++}\sin^2\frac{\theta_V}{2}(\sin^2\frac{\theta_\ell}{2} + \delta_\tau\cos\theta_\ell) + H_{--}\cos^2\frac{\theta_V}{2}(\cos^2\frac{\theta_\ell}{2} - \delta_\tau\cos\theta_\ell)\Big)$$
$$+\ 8\delta_\tau\sin\theta_\ell\sin\theta_V\cos\chi H_{t0}\Big(H_{++}\sin^2\frac{\theta_V}{2} - H_{--}\cos^2\frac{\theta_V}{2}\Big) - 8\sin\theta_V^2\cos\theta_\ell\delta_\tau H_{t0}H_{00},$$

$$\mathcal{T}_{|V_R|^2} = \sin^2\theta_V\Big(2H_{00}^2(\sin^2\theta_\ell + 2\delta_\tau\cos^2\theta_\ell) + 4\delta_\tau H_{t0}^2\Big) + 8H_{--}^2\sin^2\frac{\theta_\ell}{2}\sin^4\frac{\theta_V}{2}\Big(2\delta_\tau\cos^2\frac{\theta_\ell}{2} + \sin^2\frac{\theta_\ell}{2}\Big)$$
$$+\ 8H_{++}^2\cos^2\frac{\theta_\ell}{2}\cos^4\frac{\theta_V}{2}\Big(2\delta_\tau\sin^2\frac{\theta_\ell}{2} + \cos^2\frac{\theta_\ell}{2}\Big) + H_{++}H_{--}\sin^2\theta_\ell\sin^2\theta_V\cos 2\chi(1-2\delta_\tau)$$
$$-\ 8\sin\theta_\ell\sin\theta_V\cos\chi H_{00}\Big(H_{--}\sin^2\frac{\theta_V}{2}(\sin^2\frac{\theta_\ell}{2} + \delta_\tau\cos\theta_\ell) + H_{++}\cos^2\frac{\theta_V}{2}(\cos^2\frac{\theta_\ell}{2} - \delta_\tau\cos\theta_\ell)\Big)$$
$$+\ 8\delta_\tau\sin\theta_\ell\sin\theta_V\cos\chi H_{t0}\Big(H_{--}\sin^2\frac{\theta_V}{2} - H_{++}\cos^2\frac{\theta_V}{2}\Big) - 8\sin\theta_V^2\cos\theta_\ell\delta_\tau H_{t0}H_{00},$$

$$\mathcal{T}_{V_R^{int}} = -2\mathrm{Re}V_R\sin^2\theta_V\Big(2H_{00}^2(\sin^2\theta_\ell + 2\delta_\tau\cos^2\theta_\ell) + 4\delta_\tau H_{t0}^2\Big) - \sin^2\theta_\ell\sin^2\theta_V(1-2\delta_\tau)$$
$$\Big[H_{++}^2(\mathrm{Re}V_R\cos 2\chi + \mathrm{Im}V_R\sin 2\chi) + H_{--}^2(\mathrm{Re}V_R\cos 2\chi - \mathrm{Im}V_R\sin 2\chi)\Big]$$
$$-\ 2\mathrm{Re}V_R H_{++}H_{--}\Big[(1+\cos^2\theta_V)\big(1+\cos^2\theta_\ell + 2\delta_\tau\sin^2\theta_\ell\big) + 4\cos\theta_V\cos\theta_\ell\Big]$$
$$+\ 16\mathrm{Re}V_R\cos\theta_\ell\sin^2\theta_V H_{00}H_{t0} + \Big(4\sin\theta_V\cos\theta_\ell - \sin 2\theta_V\sin 2\theta_\ell(2\delta_\tau - 1)\Big)H_{00}$$
$$\Big(H_{++}(\mathrm{Re}V_R\cos\chi + \mathrm{Im}V_R\sin\chi) + H_{--}(\mathrm{Re}V_R\cos\chi - \mathrm{Im}V_R\sin\chi)\Big)$$
$$+\ 4\delta_\tau\sin\theta_\ell\sin 2\theta_V H_{t0}\Big[H_{++}(\mathrm{Re}V_R\cos\chi + \mathrm{Im}V_R\sin\chi) + H_{--}(\mathrm{Re}V_R\cos\chi - \mathrm{Im}V_R\sin\chi)\Big],$$

$$\mathcal{T}_{P^{int}} = 4\sqrt{2\delta_\tau}H_S^V\Big[\mathrm{Re}P\sin^2\theta_V\Big(H_{t0} - H_{00}\cos\theta_\ell\Big) + \sin\theta_V\sin\theta_\ell\Big\{H_{++}\sin^2\frac{\theta_V}{2}$$
$$\Big(\mathrm{Re}P\cos\chi + \mathrm{Im}P)\sin\chi\Big) - H_{--}\cos^2\frac{\theta_V}{2}\Big(\mathrm{Re}P\cos\chi - \mathrm{Im}P\sin\chi\Big)\Big\}\Big],$$

$$\mathcal{T}_{|T_L|^2} = 16|T_L|^2\Big[2|H_T^0|^2\sin^2\theta_V(\cos^2\theta_\ell + 2\delta_\tau\sin^2\theta_\ell) + 8|H_T^+|^2\sin^2\frac{\theta_\ell}{2}\sin^4\frac{\theta_V}{2}\Big(2\delta_\tau\sin^2\frac{\theta_\ell}{2} + \cos^2\frac{\theta_\ell}{2}\Big)$$
$$+\ 8|H_T^-|^2\cos^2\frac{\theta_\ell}{2}\cos^4\frac{\theta_V}{2}\Big(2\delta_\tau\cos^2\frac{\theta_\ell}{2} + \sin^2\frac{\theta_\ell}{2}\Big) - H_T^+H_T^-\sin^2\theta_\ell\sin^2\theta_V\cos 2\chi(1-2\delta_\tau)$$
$$-\ 4\sin\theta_\ell\sin\theta_V\cos\chi H_T^0\Big\{H_T^+\sin^2\frac{\theta_V}{2}\Big(2\delta_\tau\sin^2\frac{\theta_\ell}{2} + \cos\theta_\ell\Big) + H_T^-\cos^2\frac{\theta_V}{2}\Big(2\delta_\tau\cos^2\frac{\theta_\ell}{2} - \cos\theta_\ell\Big)\Big\}\Big],$$

$$\mathcal{T}_{T_L^{int}} = 16\sqrt{2\delta_\tau}\Big[H_T^0\Big\{\mathrm{Re}T_L\sin^2\theta_V\Big(H_{t0}\cos\theta_\ell - H_{00}\Big) + \sin\theta_\ell\sin\theta_V\Big(H_{++}\sin^2\frac{\theta_V}{2}(\mathrm{Re}T_L\cos\chi + \mathrm{Im}T_L\sin\chi)$$
$$+H_{--}\cos^2\frac{\theta_V}{2}(\mathrm{Re}T_L\cos\chi - \mathrm{Im}T_L\sin\chi)\Big)\Big\} + H_T^+\Big\{\sin\theta_\ell\sin\theta_V\Big(\mathrm{Re}T_L\cos\chi - \mathrm{Im}T_L\sin\chi\Big)$$
$$(H_{00} - H_{t0})\sin^2\frac{\theta_V}{2} - 4\mathrm{Re}T_L\sin^2\frac{\theta_\ell}{2}\sin^4\frac{\theta_V}{2}H_{++}\Big\} + H_T^-\Big\{\sin\theta_\ell\sin\theta_V\Big(\mathrm{Re}T_L\cos\chi + \mathrm{Im}T_L\sin\chi\Big)$$
$$(H_{00} + H_{t0})\cos^2\frac{\theta_V}{2} - 4\mathrm{Re}T_L\cos^2\frac{\theta_\ell}{2}\cos^4\frac{\theta_V}{2}H_{--}\Big\}\Big].$$

We only list the interference terms of NP with SM and do not show the NP-NP interference terms, but they are included in our calculations. The expressions above are now more involved for the 4-fold differential distribution and contain various combinations with θ_ℓ, θ_V and χ angles, with the imaginary couplings being proportional to $\sin\chi$. The constraints on the NP coefficients (V_L, S_L and S_R) in the 1D scenario are obtained using the condition that they are purely real. The global fit results which we consider here, do not include the vector operator V_R, as this vector operator with right-handed coupling to the quarks does not arise at the dimension-six level in the $SU(2)_L$-invariant effective theory. The relation $S_L = 4\,T_L$ in the pure imaginary case is in more agreement with the SM compared to the case with the real Wilson coefficients. However, the effects of the real and the imaginary components of these NP coefficients can be isolated by constructing different angular asymmetries.

We first consider the forward-backward asymmetry in θ_V and both θ_V, θ_ℓ with the angle χ fully integrated over:

$$
\begin{aligned}
A_{FB}^{J/\psi}(\theta_V) &= \frac{1}{\Gamma} \int dq^2 \int_0^{2\pi} d\chi \int_{-1}^1 d\cos\theta_\ell \left(\int_0^1 - \int_{-1}^0 \right) d\cos\theta_V \ \mathcal{G}[q^2, \theta_\ell, \theta_V, \chi] \\
&= \frac{8\pi}{3\Gamma} \left[|1 + V_L|^2 (1 + \delta_\ell) \left(H_{--}^2 - H_{++}^2 \right) + 8|T_L|^2 (1 + 4\delta_\ell)(|H_T^-|^2 - |H_T^+|^2) \right. \\
&\quad \left. -12\sqrt{2\delta_\ell} \left(\mathrm{Re} T_L + T_L V_L \right) \left(H_{--} H_T^- - H_{++} H_T^+ \right) \right], \\
A_{FB}^{J/\psi}(\theta_V, \theta_\ell) &= \frac{1}{\Gamma} \int dq^2 \int_0^{2\pi} d\chi \left(\int_0^1 - \int_{-1}^0 \right) d\cos\theta_V \left(\int_0^1 - \int_{-1}^0 \right) d\cos\theta_\ell \ \mathcal{G}[q^2, \theta_\ell, \theta_V, \chi] \\
&= \frac{2\pi}{\Gamma} \left[|1 + V_L|^2 \left(H_{--}^2 + H_{++}^2 \right) + 32|T_L|^2 \delta_\ell(|H_T^-|^2 + |H_T^+|^2) \right. \\
&\quad \left. -8\sqrt{2\delta_\ell} \left(\mathrm{Re} T_L + T_L V_L \right) \left(H_{++} H_T^+ + H_{--} H_T^- \right) \right],
\end{aligned}
\tag{4.2}
$$

where $\mathcal{G} = \left(\frac{d^4\Gamma}{dq^2\, d\cos\theta_\ell\, d\cos\theta_V\, d\chi} \right)$ and Γ in the denominator is the decay width of $B_c \to \mu^+ \mu^- \ell\nu_\ell$, obtained by integrating Eq. (4.1) and is given by

$$
\begin{aligned}
\Gamma(B_c \to \mu^+ \mu^- \ell\nu_\ell) &= \frac{16\pi}{9} \left[2|1 + V_L|^2 \left\{ (1 + \delta_\tau) \left(H_{00}^2 + H_{++}^2 + H_{--}^2 \right) + 3\delta_\tau H_{t0}^2 \right\} + 3|H_S^V|^2 |P|^2 \right. \\
&\quad + 6\sqrt{2\delta_\tau} H_S^V H_{t0} \left(\mathrm{Re} P + P V_L \right) + 16|T_L|^2 (1 + 4\delta_\tau) \left(|H_T^0|^2 + |H_T^+|^2 + |H_T^-|^2 \right) \\
&\quad \left. - 24\sqrt{2\delta_\tau} \left(\mathrm{Re} T_L + T_L V_L \right) \left(H_{00} H_T^0 + H_{++} H_T^+ + H_{--} H_T^- \right) \right].
\end{aligned}
\tag{4.3}
$$

It can be seen from Eq. (4.2) that the numerator is not sensitive to the scalar type NP operators. Therefore the sensitivity to the scalar NP comes only from the total decay width in the denominator, Eq. (4.3). In Fig. 10 we show $A_{FB}^{J/\psi}(\theta_V)$ and $A_{FB}^{J/\psi}(\theta_V, \theta_\ell)$ as a function of q^2 with the values of the new physics couplings as given in Eqs. (3.4, 3.5). The current bound on the NP couplings makes the observable $A_{FB}^{J/\psi}(\theta_V)$ sensitive to $S_L = 4\,T_L$ in the 1D scenario and to the same combination with both the real and the imaginary components present in case of 2D scenario. As for the asymmetry $A_{FB}^{J/\psi}(\theta_V)$, the deviation from the SM in case of 2D scenario for the combination $\mathrm{Re}[S_L = 4\,T_L]$, $\mathrm{Im}[S_L = 4\,T_L]$ can be as large as 50-70% in the region of small q^2. However, the other observable with the asymmetry in both θ_V and θ_ℓ, $A_{FB}^{J/\psi}(\theta_V, \theta_\ell)$ is not a good observable to look for NP scenarios in the current situation.

One can build additional asymmetries in the angle χ along with θ_V and θ_ℓ. These asymmetries
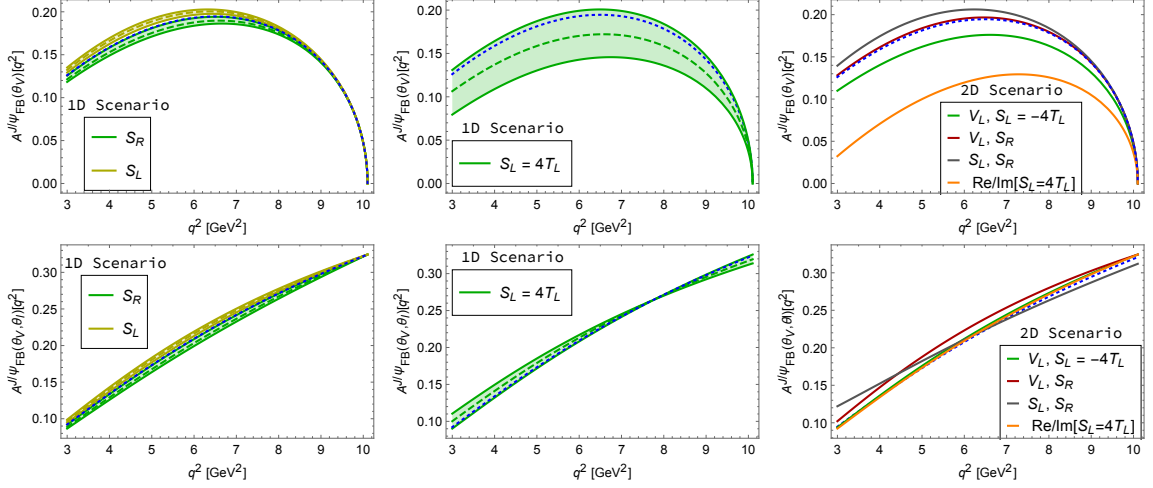
Figure 10: Forward-backward asymmetry $A^{FB}(\theta_V)$ [upper-panel] and $A^{FB}(\theta_V, \theta_\ell)$ [lower-panel] as a function of q^2. The blue dotted lines are the SM prediction, the green dashed line is for the best fit values of the NP couplings in the 1D scenario as discussed in the text. The green band represents the NP effects from the 2σ allowed regions. The third figure in both panels is the result for the best fit points in the 2D scenarios.

are proportional to both $\cos\chi$ and $\sin\chi$, and their corresponding expressions are given below:

$$
\begin{aligned}
A_{FB}^{J/\psi}(\chi, \theta_V) &= \frac{1}{\Gamma} \int dq^2 \left(\int_{-\pi/2}^{\pi/2} - \int_{\pi/2}^{3\pi/2} \right) d\chi \int_{-1}^{1} d\cos\theta_\ell \left(\int_{0}^{1} - \int_{-1}^{0} \right) d\cos\theta_V \ \mathcal{G}[q^2, \theta_\ell, \theta_V, \chi] \\
&= \frac{-4\pi}{3\Gamma} \Big[|1+V_L|^2 \Big\{ H_{00}\Big(H_{--} - H_{++}\Big) + 2\delta_\ell H_{t0}\Big(H_{--} + H_{++}\Big) \Big\} - 2H_S^V H_T^+ T_L P \\
&\quad + \sqrt{2\delta_\ell}\Big(H_{--} + H_{++}\Big) H_S^V \Big(\mathrm{Re}P + P\,V_L\Big) + 32\delta_\ell H_T^0 \Big(H_T^- - H_T^+\Big)|T_L|^2 \\
&\quad - 4\sqrt{2\delta_\ell}\Big(\mathrm{Re}T_L + T_L V_L\Big)\Big(H_{00}(H_T^- - H_T^+) + H_T^0(H_{--} - H_{++}) + H_{t0}(H_T^- + H_T^+)\Big) \Big],
\end{aligned}
$$

$$
\begin{aligned}
A_{FB}^{J/\psi}(\chi, \theta_V, \theta_\ell) &= \frac{1}{\Gamma} \int dq^2 \left(\int_{-\pi/2}^{\pi/2} - \int_{\pi/2}^{3\pi/2} \right) d\chi \left(\int_{0}^{1} - \int_{-1}^{0} \right) d\cos\theta_\ell \left(\int_{0}^{1} - \int_{-1}^{0} \right) d\cos\theta_V \ \mathcal{G}[q^2, \theta_\ell, \theta_V, \chi] \\
&= \frac{16}{9\Gamma}(2\delta_\ell - 1) \Big[|1+V_L|^2 H_{00}\Big(H_{--} + H_{++}\Big) - 16|T_L|^2 H_T^0\Big(H_T^- + H_T^+\Big) \Big]. \quad (4.4)
\end{aligned}
$$

We show in Fig. 11, the asymmetries $A_{FB}^{J/\psi}(\chi, \theta_V)$ [upper-panel] and $A^{FB}(\chi, \theta_V, \theta_\ell)$ [lower-panel] as a function of q^2. They behave similar to the asymmetries $(A_{FB}^{J/\psi}(\theta_V), A_{FB}^{J/\psi}(\theta_V, \theta_\ell))$ discussed above, where χ was integrated over the whole range. These observables do not provide any additional information compared to $A_{FB}(\theta_V)$ and $A_{FB}(\theta_V, \theta_\ell)$ discussed before. The 2D scenario in case of $A_{FB}^{J/\psi}(\chi, \theta_V)$ with $\mathrm{Re}[S_L = 4\,T_L]$, $\mathrm{Im}[S_L = 4\,T_L]$ results in about 10-20% deviation from the SM value at low values of q^2.

Finally, we consider the observables which will be sensitive to only the imaginary component of the NP operators. These asymmetries are zero within the SM. There are three possible combinations, (a) asymmetry depending only on χ, (b) asymmetry depending on χ and θ_V, and (c)
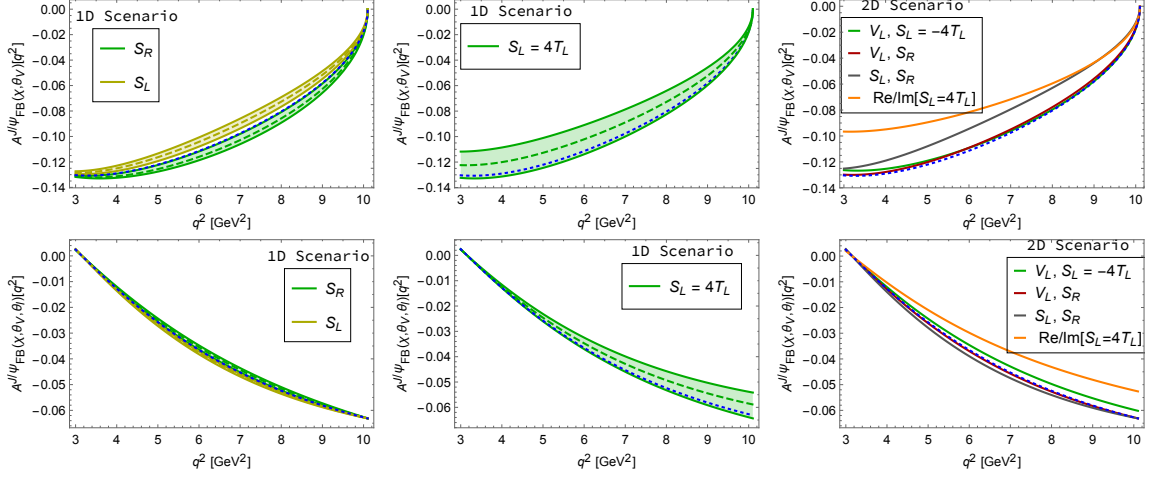
Figure 11: Asymmetries $A^{FB}(\chi, \theta_V)$ [upper-panel] and $A^{FB}(\chi, \theta_V, \theta_\ell)$ [lower-panel] as a function of q^2. The blue dotted lines are the SM prediction, the green dashed line is for the best fit values of the NP couplings in the 1D scenario as discussed in the text. The green band represents the NP effects from the 2σ allowed regions. The third figure in both panels is the result for the best fit points in the 2D scenarios.

asymmetry depending on χ, θ_V and θ_ℓ. The relevant expressions are:

$$
A^{img}_{FB}(\chi) = \frac{1}{\Gamma} \int dq^2 \left(\int_0^\pi - \int_\pi^{2\pi} \right) d\chi \int_{-1}^1 d\cos\theta_\ell \int_{-1}^1 d\cos\theta_V \; \mathcal{G}[q^2, \theta_\ell, \theta_V, \chi]
$$

$$
= \frac{\pi^2}{\Gamma} \Big[\sqrt{2\delta_\ell} \Big(4 \{ \mathrm{Im}T_L + (T_L V_L)^* \} \{ H_{00}(H_T^- - H_T^+) + H_T^0 (H_{++} - H_{--})
$$

$$
+ \; H_{t0}(H_T^+ + H_T^-) \} + H_S^V \{ \mathrm{Im}P + (P V_L)^* \} \Big(H_{--} + H_{++} \Big) \Big) + 4 H_S^V H_T^+ (P T_L)^* \Big],
$$

(4.5)

where $(T_L V_L)^* = \mathrm{Im}T_L \mathrm{Re}V_L - \mathrm{Im}V_L \mathrm{Re}T_L$, $(P V_L)^* = \mathrm{Im}P \mathrm{Re}V_L - \mathrm{Im}V_L \mathrm{Re}P$, $(P T_L)^* = \mathrm{Im}P \mathrm{Re}T_L - \mathrm{Im}T_L \mathrm{Re}P$,

$$
A^{img}_{FB}(\chi, \theta_V) = \frac{1}{\Gamma} \int dq^2 \left(\int_0^\pi - \int_\pi^{2\pi} \right) d\chi \int_{-1}^1 d\cos\theta_\ell \left(\int_0^1 - \int_{-1}^0 \right) d\cos\theta_V \; \mathcal{G}[q^2, \theta_\ell, \theta_V, \chi]
$$

$$
= \frac{4\pi}{3\Gamma} \sqrt{\delta_\ell} \Big[4\sqrt{2} \{ \mathrm{Im}T_L - (T_L V_L)^* \} \{ H_{00}(H_T^- + H_T^+) + H_{t0}(H_T^- - H_T^+) - H_T^0 (H_{++} + H_{--}) \}
$$

$$
+ \sqrt{2} H_S^V \Big(H_{--} - H_{++} \Big) \{ \mathrm{Im}P - (P V_L)^* \} + \frac{4}{\sqrt{\delta_\ell}} H_S^V H_T^+ (P T_L)^* \Big],
$$

(4.6)

$$
A^{img}_{FB}(\chi, \theta_V, \theta_\ell) = \frac{1}{\Gamma} \int dq^2 \left(\int_0^\pi - \int_\pi^{2\pi} \right) d\chi \left(\int_0^1 - \int_{-1}^0 \right) d\cos\theta_\ell \left(\int_0^1 - \int_{-1}^0 \right) d\cos\theta_V \; \mathcal{G}[q^2, \theta_\ell, \theta_V, \chi]
$$

$$
= \frac{16}{9\Gamma} (2\delta_\ell - 1) \Big[H_{00} \Big(H_{--} - H_{++} \Big) \Big(2\mathrm{Im}V_R + \mathrm{Im}V_R \mathrm{Re}V_L - \mathrm{Re}V_R \mathrm{Im}V_L \Big) \Big]. \quad (4.7)
$$

The asymmetry $A^{img}_{FB}(\chi, \theta_V, \theta_\ell)$ in only sensitive to the NP operator V_R and is therefore not relevant for our case since these V_R coefficients are not considered in the global fits as discussed before. We show in Fig. 12 $A^{img}_{FB}(\chi)$ [upper-panel] and $A^{img}_{FB}(\chi, \theta_V)$ [lower-panel] as a function of q^2. These observables are only shown for $\mathrm{Im}S_L = 4\mathrm{Im}T_L$ in the 1D scenario and $\mathrm{Re}S_L = 4\mathrm{Re}T_L$, $\mathrm{Im}S_L = 4\mathrm{Im}T_L$ in the 2D scenarios as these were the only cases considered in the global fit in Ref. [43]. The forward-backward asymmetry depending only on χ in the light of results from the current global

fit shows about 1% deviation from the SM in the 1D scenario and up to 3% deviation in the 2D scenario, in the mid-range of $q^2 = 5 - 9$ GeV^2. The asymmetry $A_{FB}^{img}(\chi, \theta_V)$ in case of the 2D scenario will have around only 1% deviation in low q^2 region, whereas it is insensitive to NP in the 1D scenario. The predictions for the integrated forward-backward asymmetries in the presence of
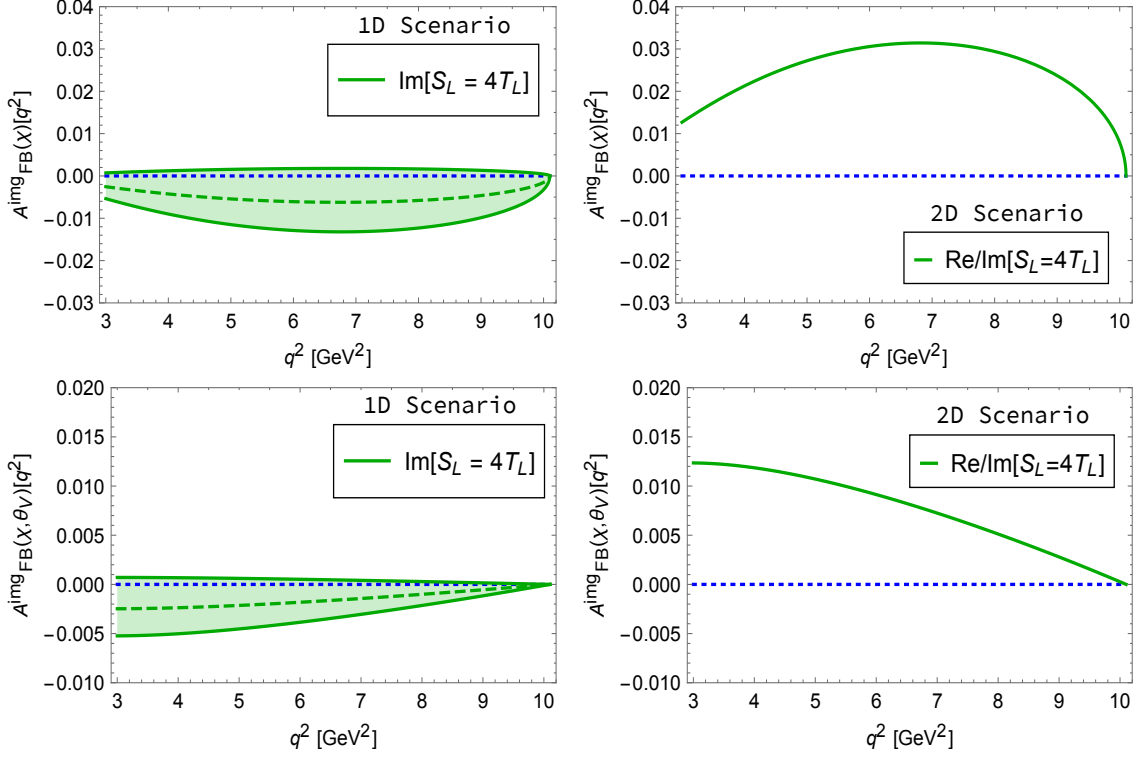

Figure 12: Asymmetries $A_{FB}^{img}(\chi)$ [upper-panel] and $A_{FB}^{img}(\chi, \theta_V)$ [lower-panel] as a function of q^2. The SM value being zero is shown by a blue dotted line, the green dashed line is for the best fit values of the NP couplings in the 1D scenario as discussed in the text. The green band represents the NP effects from the 2σ allowed regions. The second figure is for the relevant 2D scenario.

different NP operators is summarised in Table 6.

	SM	S_L	S_R	$S_L = 4T_L$	$(V_L, S_L = -4T_L)$	(S_R, S_L)	(V_L, S_R)	Re,Im$[S_L = 4T_L]$
$A_{FB}^{J/\psi}(\theta_V)$	0.16	$0.16_{0.15}^{0.16}$	$0.17_{0.16}^{0.17}$	$0.14_{0.12}^{0.17}$	0.15	0.17	0.16	0.09
$A_{FB}^{J/\psi}(\theta_V, \theta_\ell)$	0.21	$0.20_{0.20}^{0.21}$	$0.21_{0.21}^{0.22}$	$0.21_{0.21}^{0.22}$	0.21	0.22	0.21	0.21
$-A_{FB}^{J/\psi}(\chi, \theta_V)$	0.09	$0.10_{0.09}^{0.10}$	$0.09_{0.09}^{0.09}$	$0.09_{0.08}^{0.10}$	0.10	0.08	0.10	0.07
$-A_{FB}^{J/\psi}(\chi, \theta_V, \theta_\ell)$	0.03	$0.03_{0.03}^{0.03}$	$0.03_{0.03}^{0.03}$	$0.03_{0.03}^{0.03}$	0.03	0.03	0.03	0.02
$A_{img}^{FB}(\chi)$	0.0	0.0	0.0	$-0.004_{-0.01}^{0.001}$	0.0	0.0	0.0	0.02
$A_{img}^{FB}(\chi, \theta_V)$	0.0	0.0	0.0	$-0.002_{-0.003}^{0.0}$	0.0	0.0	0.0	-0.001

Table 6: The integrated values of the forward-backward asymmetries in the whole q^2 region, in case of different NP scenarios discussed in the text. The subscript and the superscript are the values for the 2σ range of the NP couplings.

5 Conclusions

Experimental measurements of semileptonic decays of the B mesons have lead to intriguing experimental tensions with the SM in the last years. The LHCb measurement of $B_c \to J/\psi l \nu_l$ decays has lead to the speculation whether the observed potential lepton flavour universality (LFU) violation in B decays can be also seen in the semileptonic B_c channels.

However, the SM prediction for the B_c decays require a knowledge of the transition form factors of $B_c \to \eta_c, J/\psi$ and the ignorance of the form factor theoretical errors yields a degree of uncertainty in the prediction. Preliminary results for these form factors exist at couple of q^2 values from the lattice QCD, but they do not cover the entire allowed range of the momentum transfer and are still given without systematical errors. We have calculated the form factors in the sum rule approach and have given the results in the full q^2 region. Our results are in good agreement with the existing lattice points. The SM branching ratios of the B_c meson to J/ψ and η_c are calculated and compared with the results from other approaches. Our predictions for the semileptonic ratios $R_{J/\psi}|_{\rm SM} = 0.23 \pm 0.01$ and $R_{\eta_c}|_{\rm SM} = 0.32 \pm 0.02$ are in agreement with other derivations and support the existing tension at 2σ level with the experiment on $R_{J/\psi}$, Eq. (1.1). With more data on B_c decays from HL-LHC all observables in $B_c \to \eta_c, J/\psi$ semileptonic decays will be within the reach of LHCb and tested in the near future.

The possible NP effects in the semileptonic decays of B_c to η_c and J/ψ is also studied based on the effective Hamiltonian approach consisting of all possible four-fermi operators. The constraints on these NP operators can be obtained from the experimental data on $R_{D(*)}$, the τ and D^* longitudinal polarization from $B \to D^*$ decay and the leptonic $B_c \to \tau\mu$ branching ratio. We take into account the latest constraints from Ref. [43] and analyse the effects of the NP operators on various observables. The ratio $R_{J/\psi}$ is sensitive to V_L in the high q^2 range whereas R_{η_c} is more sensitive to the scalar and the tensor operators, as expected.

The sensitivity of all the considered observables in this work to the different NP operators is summarized in Table 7. We find that most of the observables in the η_c decay mode are sensitive to the NP coupling S_R. The transverse polarization of τ is mostly affected by the current best fit point of the combination of coefficients Re,Im$[S_L = 4T_L]$ in the 2D NP scenario. The 2D NP scenario with the presence of both S_R, S_L leads to the largest deviation from the SM predictions for most of the observables in the case of J/ψ, apart from $R_{J/\psi}$.

	V_L	S_L	S_R	$S_L = 4T_L$	$(V_L, S_L = -4T_L)$	(S_R, S_L)	(V_L, S_R)	Re,Im$[S_L = 4T_L]$
R_{η_c}			✓					
$A_{FB}^{\eta_c}$		✓*	✓*					✓
C_F^{τ,η_c}	✓	✓		✓*				
$P_L^{\eta_c}$		✓		✓*				
$P_T^{\eta_c}$								✓
$R_{J/\psi}$	✓				✓			
$A_{FB}^{J/\psi}$						✓		
$P_L^{J/\psi}$						✓		
$P_T^{J/\psi}$				✓*		✓		✓

Table 7: Summary of the sensitivity of the observables to the NP couplings. The best fit value of the NP coupling which is most sensitive to the observable is marked with ✓. The boxes with ✓* are the ones where 2σ ranges of NP parameters give the largest deviation from the SM value.

In addition, the full 4-fold differential distribution of the decay rate $B_c \to J/\psi\ell\nu_\ell$, with J/ψ decaying to a pair of leptons of opposite helicity is considered for the first time in the presence of

new physics operators. We find that the asymmetry in the angle θ_V $(A_{FB}^{J/\psi}(\theta_V))$ is mostly sensitive to the NP couplings $\mathrm{Re},\mathrm{Im}[S_L = 4T_L]$, in the 2D NP scenarios. The asymmetries in the angle χ, which are zero in the SM and are sensitive to the imaginary part of the NP coupling, are also considered and found to be sensitive to $S_L = 4T_L$ combination of parameters. Therefore, with the current allowed parameter space for the $S_L = 4T_L$ NP parameters obtained from the global fit to experimental data on semileptonic $B \to D, D^*$ decays, the asymmetries constructed with θ_V, χ and (θ_V, χ) angles lead to significant deviation from the SM prediction.

However, it is important to stress that none of the NP scenarios derived from the recent global fit analysis of the available experimental data on semileptonic $B \to (D, D^*)\ell\nu_\ell$ decays [43] can also simultaneously explain the current 2σ tension with the experimental $R_{J/\psi}$ ratio. With the extended experimental LHCb program, future studies with more data will be needed to boost or disapprove this evidence of LFU violation in B_c decays.

Acknowledgments

A Form factors calculated in the three-point QCDSR model [4]

We have previously calculated in [4] the same form factors using a more traditional, albeit somewhat modified approach of three-point QCD sum rules (3ptQCDSR) and we present the corresponding results in Table 1. Here we just briefly discuss the method of our calculation and the main difference to the LCSR-inspired approach used in the paper. In 3ptQCDSR mesonic states are interpolated by the currents as

$$j_{B_c}(x) = \bar{c}(x)\mathrm{i}\gamma_5 b(x),$$
$$j_{J/\psi}^\nu(x) = \bar{c}(x)\gamma^\nu c(x), \tag{A.1}$$

taken at large virtualities. By inserting a set of hadronic states in the correlation function defined as

$$\Pi^{\mu\nu}(p_{B_c}, p_{J/\psi}) \equiv \mathrm{i}^2 \iint \mathrm{d}^4x\, \mathrm{d}^4y\, e^{-i(p_{B_c}x - p_{J/\psi}y)} \langle 0|T\{j_{J/\psi}^\nu(y)j_{V-A}^\mu(0)j_{B_c}^\dagger(x)\}|0\rangle, \tag{A.2}$$

one can extract the form factors by calculating the perturbative part of the correlator and the nonperturbative contributions given in terms of universal vacuum condensates built from the quark and gluon operators of increasing dimension (here we have calculated only the leading nonperturbative contribution coming from the gluon condensate) and matching the QCD result via dispersion relation to a sum over hadronic states. At the end, the expressions are Borel transformed in order to improve the convergence.

Since it is known that in the sum rule calculation of heavy meson decay constants higher orders of perturbation series can contribute as much as 40-50%, whereas the 3-point function is calculated at LO, in order to reduce the uncertainties we have performed the following procedure: in the form factors calculation we have taken for the s_0 threshold parameters the same values as those that reproduce the corresponding charmonia decay constants obtained from lattice QCD when the decay constants are calculated in the sum rules by taking into account only the LO perturbative part and the gluon-condensate contribution, i.e. with the same approximations as for the form factors,

whereas the Borel mass parameter is taken in the region where stability is achieved (we aim at the $\sim 5\%$ stability in the Borel masses in the given Borel window). Furthermore in order to reduce the uncertainties even more, we do not vary the decay constants and thresholds independently, but rather in the 3ptQCDSR calculation we always use the decay constants (varied inside the range allowed by lattice) together with the corresponding thresholds fixed by the decay constants calculation. The hope is that all the higher order/higher dimension operator contributions are then simulated through the appropriate threshold modification in the 3-point QCDSR calculation. The parameters obtained that way are given in Table 8 below. One can notice that in contrast to the LCSR-inspired calculation used in the main text, here the pole mass of the b quark is used, together with the c-quark mass derived from the ratio of masses extracted from the lattice calculations.

$m_b = 4.6^{+0.1}_{-0.1}$ GeV	$s_{B_c} = 52 - 54$ GeV^2
$m_c = Zm_b, \forall Z \approx 0.29^{+0.1}_{-0.1}$	$s_{J/\psi} = 15.5 - 16.5$ GeV^2
$\left\langle \frac{\alpha_s}{\pi} GG \right\rangle = 0.012^{+0.006}_{-0.010}$ GeV^4	$M^2_{B_c} = 60 - 80$ GeV^2
	$M^2_{J/\psi} = 20 - 25$ GeV^2

Table 8: Parameters used in the 3ptQCDSR calculation [4].

References

[1] R. Aaij *et al.* [LHCb Collaboration], "Measurement of the ratio of branching fractions $\mathcal{B}(B_c^+ \to J/\psi \tau^+ \nu_\tau)/\mathcal{B}(B_c^+ \to J/\psi \mu^+ \nu_\mu)$," Phys. Rev. Lett. **120**, no. 12, 121801 (2018) [arXiv:1711.05623 [hep-ex]].

[2] W. F. Wang, Y. Y. Fan and Z. J. Xiao, "Semileptonic decays $B_c \to (\eta_c, J/\Psi)l\nu$ in the perturbative QCD approach," Chin. Phys. C **37** (2013) 093102 [arXiv:1212.5903 [hep-ph]].

[3] V. V. Kiselev, "Exclusive decays and lifetime of B_c meson in QCD sum rules," hep-ph/0211021.

[4] D. Bečirević, D. Leljak, B. Melić and O. Sumensari, work in preparation;
talk by D. Leljak at "Getting in Grips with QCD", 4-6 April 2018, U.Paris,France,
talk by D. Bečirević at "Getting in Grips with QCD - Summer Edition", 18-22 Sept. 2018, Primošten, Croatia.

[5] T. Huang and F. Zuo, "Semileptonic B_c decays and charmonium distribution amplitude," Eur. Phys. J. C **51** (2007) 833 [hep-ph/0702147 [HEP-PH]].

[6] D. Scora and N. Isgur, "Semileptonic meson decays in the quark model: An update," Phys. Rev. D **52** (1995) 2783 [hep-ph/9503486].

[7] A. Abd El-Hady, J. H. Munoz and J. P. Vary, "Semileptonic and nonleptonic B_c decays," Phys. Rev. D **62** (2000) 014019 [hep-ph/9909406].

[8] M. A. Nobes and R. M. Woloshyn, "Decays of the B_c meson in a relativistic quark meson model," J. Phys. G **26** (2000) 1079 [hep-ph/0005056].

[9] D. Ebert, R. N. Faustov and V. O. Galkin, "Weak decays of the B_c meson to charmonium and D mesons in the relativistic quark model," Phys. Rev. D **68** (2003) 094020 [hep-ph/0306306].

[10] E. Hernandez, J. Nieves and J. M. Verde-Velasco, "Study of exclusive semileptonic and non-leptonic decays of B_c^- in a nonrelativistic quark model," Phys. Rev. D **74** (2006) 074008 [hep-ph/0607150].

[11] C. F. Qiao and R. L. Zhu, "Estimation of semileptonic decays of B_c meson to S-wave charmonia with nonrelativistic QCD," Phys. Rev. D **87** (2013) no.1, 014009 [arXiv:1208.5916 [hep-ph]].

[12] W. Wang, Y. L. Shen and C. D. Lu, "Covariant Light-Front Approach for B_c transition form factors," Phys. Rev. D **79** (2009) 054012 [arXiv:0811.3748 [hep-ph]].

[13] A. Y. Anisimov, I. M. Narodetsky, C. Semay and B. Silvestre-Brac, "The B_c meson lifetime in the light front constituent quark model," Phys. Lett. B **452** (1999) 129 [hep-ph/9812514].

[14] M. A. Ivanov, J. G. Körner and P. Santorelli, "Exclusive semileptonic and nonleptonic decays of the B_c meson," Phys. Rev. D **73** (2006) 054024 [hep-ph/0602050].

[15] J. P. Lees *et al.* [BaBar Collaboration], "Measurement of an Excess of $\bar{B} \to D^{(*)}\tau^-\bar{\nu}_\tau$ Decays and Implications for Charged Higgs Bosons," Phys. Rev. D **88**, no. 7, 072012 (2013) [arXiv:1303.0571 [hep-ex]].

[16] Y. Sato *et al.* [Belle Collaboration], "Measurement of the branching ratio of $\bar{B}^0 \to D^{*+}\tau^-\bar{\nu}_\tau$ relative to $\bar{B}^0 \to D^{*+}\ell^-\bar{\nu}_\ell$ decays with a semileptonic tagging method," Phys. Rev. D **94**, no. 7, 072007 (2016) [arXiv:1607.07923 [hep-ex]].

[17] R. Aaij *et al.* [LHCb Collaboration], "Measurement of the ratio of branching fractions $\mathcal{B}(\bar{B}^0 \to D^{*+}\tau^-\bar{\nu}_\tau)/\mathcal{B}(\bar{B}^0 \to D^{*+}\mu^-\bar{\nu}_\mu)$," Phys. Rev. Lett. **115**, no. 11, 111803 (2015) Erratum: [Phys. Rev. Lett. **115**, no. 15, 159901 (2015)] [arXiv:1506.08614 [hep-ex]].

[18] Y. Amhis *et al.* [HFLAV Collaboration], "Averages of b-hadron, c-hadron, and τ-lepton properties as of summer 2016," Eur. Phys. J. C **77**, no. 12, 895 (2017) [arXiv:1612.07233 [hep-ex]].

[19] R. Aaij *et al.* [LHCb Collaboration], "Test of lepton universality with $B^0 \to K^{*0}\ell^+\ell^-$ decays," JHEP **1708**, 055 (2017) [arXiv:1705.05802 [hep-ex]].

[20] R. Watanabe, "New Physics effect on $B_c \to J/\psi\tau\bar{\nu}$ in relation to the $R_{D^{(*)}}$ anomaly," Phys. Lett. B **776** (2018) 5 [arXiv:1709.08644 [hep-ph]].

[21] R. Dutta and A. Bhol, "$B_c \to (J/\psi, \eta_c)\tau\nu$ semileptonic decays within the standard model and beyond," Phys. Rev. D **96** (2017) no.7, 076001 [arXiv:1701.08598 [hep-ph]].

[22] T. D. Cohen, H. Lamm and R. F. Lebed, "Model-independent bounds on $R(J/\psi)$," JHEP **1809** (2018) 168 [arXiv:1807.02730 [hep-ph]].

[23] A. Berns and H. Lamm, "Model-Independent Prediction of $R(\eta_c)$," JHEP **1812**, 114 (2018) [arXiv:1808.07360 [hep-ph]].

[24] C. W. Murphy and A. Soni, "Model-Independent Determination of $B_c^+ \to \eta_c\,\ell^+\,\nu$ Form Factors," Phys. Rev. D **98**, no. 9, 094026 (2018) [arXiv:1808.05932 [hep-ph]].

[25] C. T. Tran, M. A. Ivanov, J. G. Körner and P. Santorelli, "Implications of new physics in the decays $B_c \to (J/\psi, \eta_c)\tau\nu$," Phys. Rev. D **97** (2018) no.5, 054014 [arXiv:1801.06927 [hep-ph]].

[26] B. Colquhoun *et al.* [HPQCD Collaboration], "B_c decays from highly improved staggered quarks and NRQCD," PoS LATTICE **2016** (2016) 281 [arXiv:1611.01987 [hep-lat]].

[27] P. Ball and V. M. Braun, "The ρ meson light cone distribution amplitudes of leading twist revisited," Phys. Rev. D **54**, 2182 (1996) [hep-ph/9602323].

[28] G. Duplančić and B. Melić, "$B, B_s \to K$ form factors: An Update of light-cone sum rule results," Phys. Rev. D **78**, 054015 (2008) [arXiv:0805.4170 [hep-ph]].

[29] P. Ball and R. Zwicky, "$B_{d,s} \to \rho, \omega, K^*, \phi$ decay form-factors from light-cone sum rules revisited," Phys. Rev. D **71** (2005) 014029 [hep-ph/0412079].

[30] G. Duplančić, A. Khodjamirian, T. Mannel, B. Melić and N. Offen, "Light-cone sum rules for $B \to \pi$ form factors revisited," JHEP **0804**, 014 (2008) [arXiv:0801.1796 [hep-ph]].

[31] G. Duplančić and B. Melić, "Form factors of $B, B_s \to \eta'$ and $D, D_s \to \eta'$ transitions from QCD light-cone sum rules," JHEP **1511**, 138 (2015) [arXiv:1508.05287 [hep-ph]].

[32] A. Khodjamirian, C. Klein, T. Mannel and Y.-M. Wang, "Form Factors and Strong Couplings of Heavy Baryons from QCD Light-Cone Sum Rules," JHEP **1109**, 106 (2011) [arXiv:1108.2971 [hep-ph]].

[33] G. Bell, T. Feldmann, Y. M. Wang and M. W. Y. Yip, "Light-Cone Distribution Amplitudes for Heavy-Quark Hadrons," JHEP **1311**, 191 (2013) [arXiv:1308.6114 [hep-ph]].

[34] B. Chauhan and B. Kindra, "Invoking Chiral Vector Leptoquark to explain LFU violation in B Decays," arXiv:1709.09989 [hep-ph].

[35] X. G. He and G. Valencia, "Lepton universality violation and right-handed currents in $b \to c\tau\nu$," Phys. Lett. B **779**, 52 (2018) [arXiv:1711.09525 [hep-ph]].

[36] J. Zhu, B. Wei, J. H. Sheng, R. M. Wang, Y. Gao and G. R. Lu, "Probing the R-parity violating supersymmetric effects in in $B_c \to J/\psi \ell^- \bar{\nu}_\ell, \eta_c \ell^- \bar{\nu}_\ell$ and $\Lambda_b \to \Lambda_c \ell^- \bar{\nu}_\ell$ decays," Nucl. Phys. B **934**, 380 (2018) [arXiv:1801.00917 [hep-ph]].

[37] A. Biswas, D. K. Ghosh, S. K. Patra and A. Shaw, "$b \to c\ell\nu$ anomalies in light of extended scalar sectors," arXiv:1801.03375 [hep-ph].

[38] R. Dutta, "Exploring R_D, R_{D^*} and $R_{J/\Psi}$ anomalies," arXiv:1710.00351 [hep-ph].

[39] Z. R. Huang, Y. Li, C. D. Lu, M. A. Paracha and C. Wang, "Footprints of New Physics in $b \to c\tau\nu$ Transitions," Phys. Rev. D **98**, no. 9, 095018 (2018) [arXiv:1808.03565 [hep-ph]].

[40] Y. Li and C. D. L, "Recent Anomalies in B Physics," Sci. Bull. **63**, 267 (2018) [arXiv:1808.02990 [hep-ph]].

[41] R. Alonso, A. Kobach and J. Martin Camalich, "New physics in the kinematic distributions of $\bar{B} \to D^{(*)} \tau^- (\to \ell^- \bar{\nu}_\ell \nu_\tau) \bar{\nu}_\tau$," Phys. Rev. D **94** (2016) no.9, 094021 [arXiv:1602.07671 [hep-ph]].

[42] A. Greljo, J. Martin Camalich and J. D. Ruiz-Álvarez, "The Mono-Tau Menace: From B Decays to High-p_T Tails," arXiv:1811.07920 [hep-ph].

[43] M. Blanke, A. Crivellin, S. de Boer, M. Moscati, U. Nierste, I. Nišandžić and T. Kitahara, "Impact of polarization observables and $B_c \to \tau\nu$ on new physics explanations of the $b \to c\tau\nu$ anomaly," arXiv:1811.09603 [hep-ph].

[44] F. Feruglio, P. Paradisi and O. Sumensari, "Implications of scalar and tensor explanations of $R_{D^{(*)}}$," JHEP **1811**, 191 (2018) [arXiv:1806.10155 [hep-ph]].

[45] A. K. Alok, D. Kumar, J. Kumar, S. Kumbhakar and S. U. Sankar, JHEP **1809**, 152 (2018) doi:10.1007/JHEP09(2018)152 [arXiv:1710.04127 [hep-ph]].

[46] A. K. Alok, D. Kumar, S. Kumbhakar and S. Uma Sankar, Phys. Lett. B **784**, 16 (2018) doi:10.1016/j.physletb.2018.07.001 [arXiv:1804.08078 [hep-ph]].

[47] G. T. Bodwin, H. S. Chung, D. Kang, J. Lee and C. Yu, "Improved determination of color-singlet nonrelativistic QCD matrix elements for S-wave charmonium," Phys. Rev. D **77**, 094017 (2008) [arXiv:0710.0994 [hep-ph]].

[48] A. Bharucha, D. M. Straub and R. Zwicky, "$B \to V\ell^+\ell^-$ in the Standard Model from light-cone sum rules," JHEP **1608** (2016) 098 [arXiv:1503.05534 [hep-ph]].

[49] V. M. Braun, A. Khodjamirian and M. Maul, "Pion form-factor in QCD at intermediate momentum transfers," Phys. Rev. D **61**, 073004 (2000) [hep-ph/9907495].

[50] P. Ball and R. Zwicky, "Improved analysis of $B \to \pi e\nu$ from QCD sum rules on the light cone," JHEP **0110**, 019 (2001) [hep-ph/0110115].

[51] P. Ball and R. Zwicky, "New results on $B \to \pi, K, \eta$ decay formfactors from light-cone sum rules," Phys. Rev. D **71**, 014015 (2005) [hep-ph/0406232].

[52] A. Khodjamirian, T. Mannel, N. Offen and Y.-M. Wang, "$B \to \pi\ell\nu_l$ Width and $|V_{ub}|$ from QCD Light-Cone Sum Rules," Phys. Rev. D **83**, 094031 (2011) [arXiv:1103.2655 [hep-ph]].

[53] P. Ball and V. M. Braun, "Exclusive semileptonic and rare B meson decays in QCD," Phys. Rev. D **58**, 094016 (1998) [hep-ph/9805422].

[54] W. Altmannshofer, P. Ball, A. Bharucha, A. J. Buras, D. M. Straub and M. Wick, "Symmetries and Asymmetries of $B \to K^* \mu^+ \mu^-$ Decays in the Standard Model and Beyond," JHEP **0901**, 019 (2009) [arXiv:0811.1214 [hep-ph]].

[55] V. L. Chernyak and A. R. Zhitnitsky, "Asymptotic Behavior of Exclusive Processes in QCD," Phys. Rept. **112** (1984) 173.

[56] C. McNeile, C. T. H. Davies, E. Follana, K. Hornbostel and G. P. Lepage, "High-Precision c and b Masses, and QCD Coupling from Current-Current Correlators in Lattice and Continuum QCD," Phys. Rev. D **82** (2010) 034512 [arXiv:1004.4285 [hep-lat]].

[57] C. McNeile, C. T. H. Davies, E. Follana, K. Hornbostel and G. P. Lepage, "Heavy meson masses and decay constants from relativistic heavy quarks in full lattice QCD," Phys. Rev. D **86** (2012) 074503 [arXiv:1207.0994 [hep-lat]].

[58] G. C. Donald, C. T. H. Davies, R. J. Dowdall, E. Follana, K. Hornbostel, J. Koponen, G. P. Lepage and C. McNeile, "Precision tests of the J/ψ from full lattice QCD: mass, leptonic width and radiative decay rate to η_c," Phys. Rev. D **86**, 094501 (2012) [arXiv:1208.2855 [hep-lat]].

[59] C. T. H. Davies, C. McNeile, E. Follana, G. P. Lepage, H. Na and J. Shigemitsu, "Update: Precision D_s decay constant from full lattice QCD using very fine lattices," Phys. Rev. D **82** (2010) 114504 [arXiv:1008.4018 [hep-lat]].

[60] D. Bečirević, G. Duplančić, B. Klajn, B. Melić and F. Sanfilippo, "Lattice QCD and QCD sum rule determination of the decay constants of η_c, J/ψ and h_c states," Nucl. Phys. B **883** (2014) 306 [arXiv:1312.2858 [hep-ph]].

[61] G. T. Bodwin, E. Braaten and G. P. Lepage, "Rigorous QCD analysis of inclusive annihilation and production of heavy quarkonium," Phys. Rev. D **51**, 1125 (1995) [Erratum-ibid. D **55**, 5853 (1997)] [hep-ph/9407339].

[62] V. V. Braguta, A. K. Likhoded and A. V. Luchinsky, "The Study of leading twist light cone wave function of η_c meson," Phys. Lett. B **646** (2007) 80 [hep-ph/0611021].

[63] V. V. Braguta, "The study of leading twist light cone wave functions of J/ψ meson," Phys. Rev. D **75** (2007) 094016 [hep-ph/0701234 [hep-ph]].

[64] Y. Grossman, M. König and M. Neubert, "Exclusive Radiative Decays of W and Z Bosons in QCD Factorization," JHEP **1504** (2015) 101 [arXiv:1501.06569 [hep-ph]].

[65] A. Czarnecki and K. Melnikov, "Two loop QCD corrections to the heavy quark pair production cross-section in e^+e^- annihilation near the threshold," Phys. Rev. Lett. **80**, 2531 (1998) [hep-ph/9712222].

[66] M. Beneke, A. Signer and V. A. Smirnov, "Two loop correction to the leptonic decay of quarkonium," Phys. Rev. Lett. **80**, 2535 (1998) [hep-ph/9712302].

[67] M. Beneke, Y. Kiyo, P. Marquard, A. Penin, J. Piclum, D. Seidel and M. Steinhauser, "Leptonic decay of the $\Upsilon(1S)$ meson at third order in QCD," Phys. Rev. Lett. **112**, 151801 (2014) [arXiv:1401.3005 [hep-ph]].

[68] X. P. Wang and D. Yang, "The leading twist light-cone distribution amplitudes for the S-wave and P-wave quarkonia and their applications in single quarkonium exclusive productions," JHEP **1406** (2014) 121 [arXiv:1401.0122 [hep-ph]].

[69] W. Wang, J. Xu, D. Yang and S. Zhao, "Relativistic corrections to light-cone distribution amplitudes of S-wave B_c mesons and heavy quarkonia," JHEP **1712** (2017) 012 [arXiv:1706.06241 [hep-ph]].

[70] H. S. Chung, J. Lee and C. Yu, "NRQCD matrix elements for S-wave bottomonia and $\Gamma(\eta_b(nS) \to \gamma\gamma)$ with relativistic corrections," Phys. Lett. B **697**, 48 (2011) [arXiv:1011.1554 [hep-ph]].

[71] G. T. Bodwin, H. S. Chung, J. H. Ee, J. Lee and F. Petriello, "Relativistic corrections to Higgs boson decays to quarkonia," Phys. Rev. D **90**, no. 11, 113010 (2014) [arXiv:1407.6695 [hep-ph]].

[72] P. Ball, V. M. Braun and A. Lenz, "Higher-twist distribution amplitudes of the K meson in QCD," JHEP **0605**, 004 (2006) [hep-ph/0603063].

[73] P. Ball, V. M. Braun, Y. Koike and K. Tanaka, "Higher twist distribution amplitudes of vector mesons in QCD: Formalism and twist - three distributions," Nucl. Phys. B **529**, 323 (1998) [hep-ph/9802299].

[74] P. Ball and V. M. Braun, "Handbook of higher twist distribution amplitudes of vector mesons in QCD," hep-ph/9808229.

[75] M. Beneke and T. Feldmann, "Symmetry breaking corrections to heavy to light B meson form-factors at large recoil," Nucl. Phys. B **592** (2001) 3 [hep-ph/0008255].

[76] P. Ball, V. M. Braun and A. Lenz, "Twist-4 distribution amplitudes of the K^* and φ mesons in QCD," JHEP **0708** (2007) 090 [arXiv:0707.1201 [hep-ph]].

[77] A. Issadykov, M. A. Ivanov and G. Nurbakova, "Semileptonic decays of B_c mesons into charmonium states," EPJ Web Conf. **158** (2017) 03002.

[78] C. Bourrely, I. Caprini and L. Lellouch, "Model-independent description of $B \to \pi l \nu$ decays and a determination of $|V_{ub}|$," Phys. Rev. D **79** (2009) 013008 Erratum: [Phys. Rev. D **82** (2010) 099902] [arXiv:0807.2722 [hep-ph]].

[79] A. Bharucha, T. Feldmann and M. Wick, "Theoretical and Phenomenological Constraints on Form Factors for Radiative and Semi-Leptonic B-Meson Decays," JHEP **1009** (2010) 090 [arXiv:1004.3249 [hep-ph]].

[80] G. Aad *et al.* [ATLAS Collaboration], "Observation of an Excited $B_c^\pm$ Meson State with the ATLAS Detector," Phys. Rev. Lett. **113**, no. 21, 212004 (2014) [arXiv:1407.1032 [hep-ex]].

[81] R. Aaij *et al.* [LHCb Collaboration], "Observation of $B_c^+ \to J/\psi D^{(*)} K^{(*)}$ decays," Phys. Rev. D **95**, no. 3, 032005 (2017) [arXiv:1612.07421 [hep-ex]].

[82] E. J. Eichten and C. Quigg, "Mesons with beauty and charm: Spectroscopy," Phys. Rev. D **49**, 5845 (1994) [hep-ph/9402210].

[83] S. Godfrey, "Spectroscopy of B_c mesons in the relativized quark model," Phys. Rev. D **70**, 054017 (2004) [hep-ph/0406228].

[84] E. E. Jenkins, M. E. Luke, A. V. Manohar and M. J. Savage, "Semileptonic B_c decay and heavy quark spin symmetry," Nucl. Phys. B **390**, 463 (1993) [hep-ph/9204238].

[85] V. V. Kiselev, A. K. Likhoded and A. I. Onishchenko, "Semileptonic B_c meson decays in sum rules of QCD and NRQCD," Nucl. Phys. B **569**, 473 (2000) [hep-ph/9905359].

[86] P. Colangelo and F. De Fazio, "Using heavy quark spin symmetry in semileptonic B_c decays," Phys. Rev. D **61**, 034012 (2000) [hep-ph/9909423].

[87] M. Tanabashi *et al.* [Particle Data Group], "Review of Particle Physics," Phys. Rev. D **98**, no. 3, 030001 (2018).

[88] M. Beneke and G. Buchalla, "The B_c Meson Lifetime," Phys. Rev. D **53**, 4991 (1996) [hep-ph/9601249].

[89] A. Angelescu, D. Bečirević, D. A. Faroughy and O. Sumensari, "Closing the window on single leptoquark solutions to the B-physics anomalies," JHEP **1810**, 183 (2018) [arXiv:1808.08179 [hep-ph]].

[90] I. Doršner, S. Fajfer, A. Greljo, J. F. Kamenik and N. Košnik, "Physics of leptoquarks in precision experiments and at particle colliders," Phys. Rept. **641**, 1 (2016) [arXiv:1603.04993 [hep-ph]].

[91] D. Bečirević, S. Fajfer, N. Košnik and O. Sumensari, "Leptoquark model to explain the B-physics anomalies, R_K and R_D," Phys. Rev. D **94**, no. 11, 115021 (2016) [arXiv:1608.08501 [hep-ph]].

[92] M. González-Alonso, J. Martin Camalich and K. Mimouni, "Renormalization-group evolution of new physics contributions to (semi)leptonic meson decays," Phys. Lett. B **772**, 777 (2017) [arXiv:1706.00410 [hep-ph]].

[93] M. A. Ivanov, J. G. Körner and C. T. Tran, "Analyzing new physics in the decays $\bar{B}^0 \to D^{(*)}\tau^-\bar{\nu}_\tau$ with form factors obtained from the covariant quark model," Phys. Rev. D **94**, no. 9, 094028 (2016) [arXiv:1607.02932 [hep-ph]].

[94] T. D. Cohen, H. Lamm and R. F. Lebed, "Tests of the standard model in $B \to Dl\nu_l$, $B \to D^*l\nu_l$ and $B_c \to J/\psi l\nu_l$," Phys. Rev. D **98** (2018) no.3, 034022 [arXiv:1807.00256 [hep-ph]].

[95] A. Faessler, T. Gutsche, M. A. Ivanov, J. G. Körner, and V. E. Lyubovitskij, "The Exclusive rare decays $B \to K(K*) \, \bar{\ell}\ell$ and $B_c \to D(D*) \, \bar{\ell}\ell$ in a relativistic quark model," Eur. Phys. J. direct C **4**, 18 (2002), arXiv:hep-ph/0205287.

[96] T. Gutsche, M. A. Ivanov, J. G. Körner, V. E. Lyubovitskij, and P. Santorelli, "Polarization effects in the cascade decay $\Lambda_b \to \Lambda(\to p\pi^-) + J/\psi(\to l^+l^-)$ in the covariant confined quark model," Phys. Rev. D **88**, 114018 (2013), arXiv:1309.7879.

[97] T. Gutsche, M. A. Ivanov, J. G. Körner, V. E. Lyubovitskij, P. Santorelli, and N. Habyl, "Semileptonic decay $\Lambda_b \to \Lambda_c + \tau^- + \bar{\nu}_\tau$ in the covariant confined quark model," Phys. Rev. D **91**, 074001 (2015); **91**, 119907(E) (2015), arXiv:1502.04864.